Journal Pre-proof

Design, synthesis and biological evaluation of indole-2-carboxylic acid derivatives as IDO1/TDO dual inhibitors

Guonan Cui, Fangfang Lai, Xiaoyu Wang, Xiaoguang Chen, Bailing Xu

PII: S0223-5234(19)31137-7

DOI: https://doi.org/10.1016/j.ejmech.2019.111985

Reference: EJMECH 111985

To appear in: *European Journal of Medicinal Chemistry*

Received Date: 17 October 2019

Revised Date: 4 December 2019

Accepted Date: 17 December 2019

Please cite this article as: G. Cui, F. Lai, X. Wang, X. Chen, B. Xu, Design, synthesis and biological evaluation of indole-2-carboxylic acid derivatives as IDO1/TDO dual inhibitors, *European Journal of Medicinal Chemistry* (2020), doi: https://doi.org/10.1016/j.ejmech.2019.111985.

Graphical Abstract:

Design, synthesis and biological evaluation of indole-2-carboxylic acid derivatives as IDO1/TDO dual inhibitors

Guonan Cui, Fangfang Lai, Xiaoyu Wang, Xiaoguang Chen, Bailing Xu

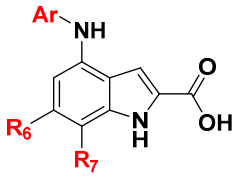

The indole-2-carboxylic acid derivatives were disclosed as novel IDO1/TDO dual inhibitors.

Design, synthesis and biological evaluation of indole-2-carboxylic acid derivatives as IDO1/TDO dual inhibitors

Guonan Cui[a,#], Fangfang Lai[b,#], Xiaoyu Wang[a], Xiaoguang Chen[b,*], Bailing Xu[a,*]

[a]*Beijing Key Laboratory of Active Substance Discovery and Druggability Evaluation, Institute of Materia Medica, Chinese Academy of Medical Sciences &Peking Union Medical College, Beijing, 100050, China*

[b]*State Key Laboratory of Bioactive Substances and Functions of Natural Medicines, Institute of Materia Medica, Chinese Academy of Medical Sciences &Peking Union Medical College, Beijing, 100050, China*

Abstract

Indoleamine 2,3-dioxygenase 1 (IDO1) and tryptophan 2,3-dioxygenase (TDO) are involved in the key steps of tryptophan metabolism and are potential new targets for tumor immunotherapy. In this work, a variety of indole-2-carboxylic acid derivatives were synthesized, and their inhibitory activities against both enzymes along with structure-activity relationships were investigated. As a result, a number of 6-acetamido-indole-2-carboxylic acid derivatives were found to be potent dual inhibitors with IC_{50} values at low micromolar levels. Among them, compound **9o-1** was the most potent inhibitor with an IC_{50} value of 1.17 μM for IDO1, and 1.55 μM for TDO, respectively. In addition, a para-benzoquinone derivative **9p-O**, resulted from the oxidation of compound **9p**, was also identified and it showed strong inhibition against the two enzymes with IC_{50} values at the double digit nanomolar level. Using molecular docking and molecular dynamic simulations, we predicted the binding modes of this class of compounds within IDO1 and TDO binding pocket. The results provide insights for further structural optimization of this series of IDO1/TDO dual inhibitors.

Keywords: indoleamine 2,3-dioxygenase 1, tryptophan 2,3-dioxygenase, indole-2-carboxylic acid, dual inhibitors

# The first two authors contributed equally.
* Corresponding author. Bailing Xu, Tel: +86 10 63166764; Xiaoguang Chen, Tel: +86 10 63166302
E-mail address: xubl@imm.ac.cn (B. Xu); chxg@imm.ac.cn (X. Chen).

1. Introduction

Indoleamine 2,3-dioxygenase 1 (IDO1) and tryptophan 2,3-dioxygenase (TDO) are heme-containing enzymes that catalyze the first and rate-limiting step of tryptophan catabolism along the kynurenine pathway, generating tryptophan dioxide, which was converted to *N*-formyl kynurenine and kynurenine derivatives [1]. IDO1 and TDO are found to be overexpressed in various cancer cells with different levels [2, 3]. In the tumor microenvironment, tryptophan depletion and kynurenine metabolites accumulation led to the enhancement of the number and function of Tregs cells [4] and inhibition of effector T-cells [5]. These two mechanisms are synergistic to immunosuppress, helping cancer cells to escape a potentially effective immune response [2, 6]. These discoveries have triggered a great deal of new interest in targeting TDO and IDO for drug discovery.

Although IDO1 and TDO have similar biological roles, their distribution is different. IDO1 is an extrahepatic cytosolic enzyme that is distributed in various tissues, including placenta, lung, liver, spleen, kidney, stomach, large intestine, small intestine and colon, playing a key role in the tryptophan oxidative cleavage reaction [1, 7]; TDO is mainly expressed in the liver, controlling the concentration of tryptophan in the blood [1]. There is also a large difference in the structure between IDO1 and TDO. IDO1 is a monomeric enzyme, and TDO is a homotetrameric enzyme. However, their active sites are highly similar, though their sequence identity is only 16% [8, 9]. Furthermore, TDO exhibited high substrate specificity and catalyzed the oxidative cleavage of Trp preferentially. In contrast, IDO1 showed greater substrate promiscuity than TDO, and a range of indoleamines including Trp, serotonin and tryptamine could be catabolized by IDO1 [10].

At present, many pharmaceutical companies and research institutes have conducted extensive studies on IDO1 inhibition [11-31]. And numerous structurally distinct chemical entities were disclosed, and this inhibitor structure diversity along with its substrate promiscuity likely resulted from the flexibility of the active site within IDO1 in part [25]. For the present, several IDO1 inhibitors have advanced into

clinical trials such as Epacadostat [26, 27], BMS986205 [28], Indoximod [29], PF-0684003 [30] and Navoximod [31]. Compared with inhibitors of IDO1, there are few studies on TDO inhibitors [32-37], and no inhibitors enter the clinical trial. However, the current clinical results of IDO1 inhibitors are not very satisfying. Epacadostat combined with PD-1 checkpoint inhibitor pembrolizumab for the treatment of unresectable or metastatic melanoma, no significant improvement in progression-free survival rate (PFS) was observed compared with pembrolizumab alone [38]. It is speculated that selective inhibition of IDO1 has limited effects on tumor growth, probably due to inhibition of IDO1 leading to TDO activation in tumors, which compensates for the increased ratio of Trp/Kyn caused by IDO1 inhibition. Therefore, The IDO1/TDO dual inhibitors may become a new strategy for tumor immunotherapy [39, 40].

A random screening of our in-house compound library, which featured an indole scaffold, was conducted. And indole-2-carboxylic acid compounds **9a** and **9k** were found to be the dual inhibitors with a novel scaffold, although these two hits displayed weak inhibitory activity against both IDO1 and TDO. Thus, we took compounds **9a** and **9k** as the starting point to embark on extensive structural modifications with an aim to search for novel IDO1/TDO dual inhibitors with improved potency. Herein, the chemical synthesis of these derivatives and the investigation on the structure-activity relationships were reported.

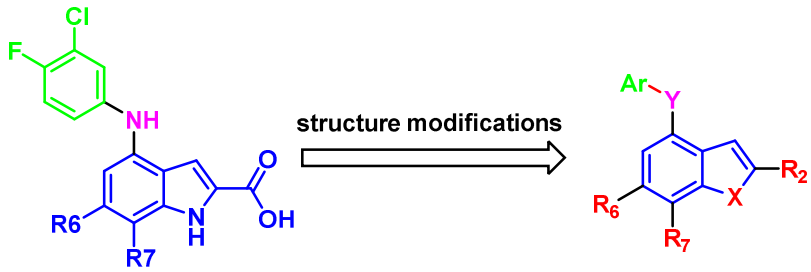

9a R_6 = H, R_7 = F, IC_{50} = 40.7 μM (IDO1), IC_{50} = 99.2 μM (TDO)
9k R_6 = CH_3, R_7 = H, IC_{50} = 35.6 μM (IDO1), IC_{50} = 22.5 μM (TDO)

Figure 1. The structures of the hits **9a, 9k** and the general structure of designed derivatives

2. Results and discussion

2.1 Chemistry

Two methods were used to construct the key intermediates 4-bromo-1*H*-indole-2-carboxylate derivatives as shown in **scheme 1**. The Hemetsberger's method was utilized to produce compounds **3a**, **3c-3f** and **3i-3m**. In the presence of strong base sodium ethoxide, the substituted benzaldehydes (**1a, 1c-1f**, **1i-1m**) were condensed with ethyl azidoacetate to form alkenyl azides **2** with yields of 12-42%. Compounds **2** were heated to 180 ℃ to afford 4-bromo-indole intermediates **3** in 30-93% yields. Compounds **3g** and **3n** were prepared using Fisher indole synthesis method. It was noted that compound **6n** was cyclized using PPA as the solvent to give rise to two isomers. The ^{1}H-NMR spectroscopy confirms that the two isomers were respectively ethyl 4-nitro-6-bromide-1*H*-indole- 2-carboxylate ($\delta_{H\text{-}7}$ 7.93 ppm, 49.4%) and the desired ethyl 4-bromo-6-nitro-1*H*-indole-2-carboxylate (**3n**, $\delta_{H\text{-}7}$ 8.38 ppm, 33.1%). The nitro group of **3n** was reduced and acetylated to provide 6-acetamido-4-bromo-indole intermediate **3o**.

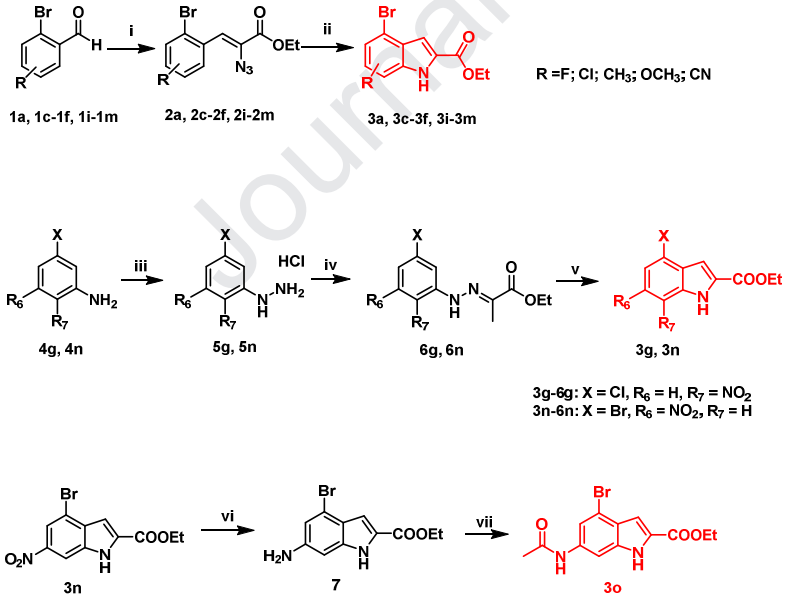

Scheme 1. Reagents and conditions: (i) NaOEt, ethyl azidoacetate, ethyl trifluoroacetate, EtOH, 12.0%-42.3%. (ii) 1,2-dichlorobenzene, reflux, 30.0%-93.0%. (iii) $NaNO_2$, $SnCl_2$, HCl, H_2O, -30 ℃, 89.2%-99.0%. (iv) ethyl 2-oxopropanoate, r.t., 37.0%-82.8%. (v) PPA, 80 ℃, 30.0%-33.1%. (vi) Fe, NH_4Cl, EtOH and H_2O, 80 ℃, 86%. (vii) CH_3COCl, TEA, DMF, r.t., 96.6%.

As shown in **scheme 2**, the majority of target compounds **9** were constructed via two steps starting from the key intermediates **3**. 4-Bromo-substituted indole derivatives **3** were subjected to a variety of aryl amines under the condition of Buchwald-Hartwig cross coupling reaction to prepare aryl indole amines **8** in the yield of 26-91%, which were hydrolyzed under basic conditions, providing target compounds **9a-9g**, **9i-9o**, **9a-1-9a-17** and **9o-1-9o-24**. By using iron powder and ammonium chloride, the 7-nitro-substituted intermediate **8g** was reduced and acylated to generate compound **8h,** which was subjected to hydrolysis to give the target compound **9h** with a 7-acetamido group on the indole ring. The target compound **9p** with a 6-ethylamine was obtained by reduction of 6-acetamido-substituted compound **8o** and hydrolysis. Starting from compounds **8a** and **8k,** the *N*-1 methyl substituted compounds **9q** and **9r** were readily prepared by methylation and ester hydrolysis in high yields. Compound **11** was a key substrate for the preparation of benzothiophene derivative **3s**. Starting from 4-acetamidobenzaldehyde **10**, 2-aminobenzoic acid was reacted with an aldehyde group to form an imine as a transient directing group, which was further subjected to Pd (II)-catalyzed ortho-C-H chlorination in the presence of $Pd(OAc)_2$, AgTFA and NCS to achieve the dichloro substituted aldehyde compound **11** in 57.8% yield [41]. Then compound **11** was reacted with ethyl thioglycolate in the presence of K_2CO_3 to form the benzothiophene intermediate **3s**, which was converted into target compound **9s** by coupling and hydrolysis reaction.

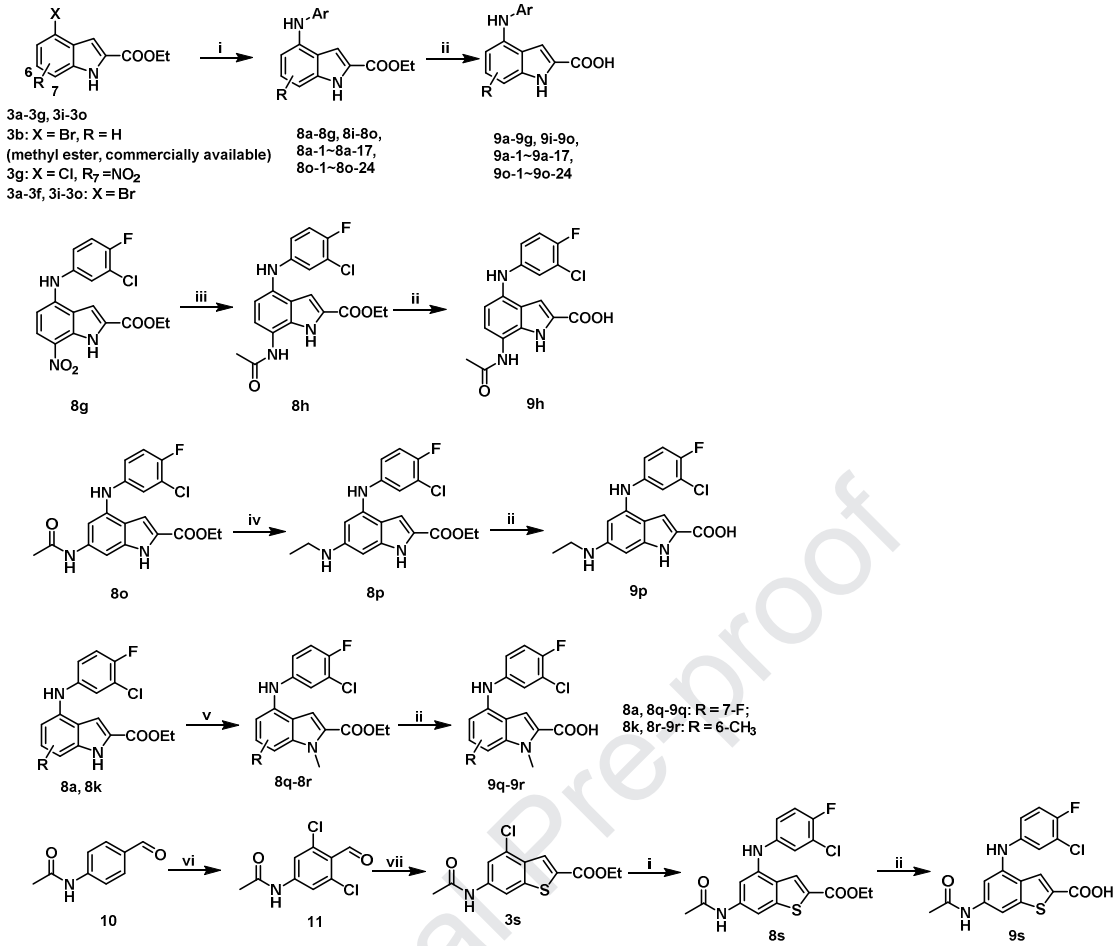

Scheme 2. Reagents and conditions: (i) aryl amine, $Pd_2(dba)_3$, DavePhos, K_3PO_4(aq), toluene, 80 □; aryl amine, $Pd_2(dba)_3$, XantPhos, Na_2CO_3(aq), toluene, reflux; aryl amine, $Pd_2(dba)_3$, X-phos, Cs_2CO_3, 1,4-dioxane, 100 □; aryl amine, $Pd_2(dba)_3$, Xantphos, Cs_2CO_3, 1,4-dioxane, 100 □, 25.9%-90.7%. (ii) NaOH, THF, EtOH and H_2O, r.t.; LiOH, THF, EtOH and H_2O, 40 □; Na_2CO_3, EtOH and H_2O, reflux, 23.8%-99.7%. (iii) Fe, NH_4Cl, EtOH and H_2O, 80 □, 54.9%; CH_3COCl, DIEA, DCM, r.t., 58.9%. (iv) BH_3·THF, THF, 0 □~r.t., 39.9%. (v) CH_3I, K_2CO_3, DMF, 97.5%-98.6%. (vi) NCS, $Pd(OAc)_2$, Ag(TFA), 2-aminobenzoic acid, TFA, DCE, 60 □, 57.8%. (vii) K_2CO_3, ethyl thioglycolate, DMF, 60 □, 62.4%.

The variation of the substituents on the 2-position of indole ring was performed and the synthesis of the corresponding compounds **14a-14g** was depicted in **Scheme 3**. 2-Methyl substituted compound **14a** was constructed by two steps reaction. Using the Bartoli indole synthesis method, 2-fluoro-5-bromonitrobenzene **12** and isopropenyl magnesium bromide reacted at low temperature to yield 2-methyl-4-bromo-7-fluoro-1*H*-indole **13**, which was transformed into the target product **14a** by a coupling reaction. Upon treatment of 2-carboxyl acid substituted compound **9a** with Cu powder and quinolone as a solvent, compound **14b** was obtained in 46.5% yield through a decarboxylation reaction at a high temperature.

Upon treatment of compound **9a** with borane in THF solution, 2-hydroxymethyl-substituted compound **14c** was resulted in 55.7% yield. Compounds **14d** and **14e** were prepared by condensation reaction of compound **9a** with ammonium hydroxide and hydroxylamine, respectively. Utilizing a series of hydrolysis, condensation and dehydration reaction, compound **3a** was converted into 2-cyano-4-bromo-7-fluoroindole **15**, which was then coupled with 3-chloro-4-fluoroaniline to give compound **14f**. Subsequently, compound **14f** was transformed into the target compound **14g** in the presence of hydroxylamine and TEA.

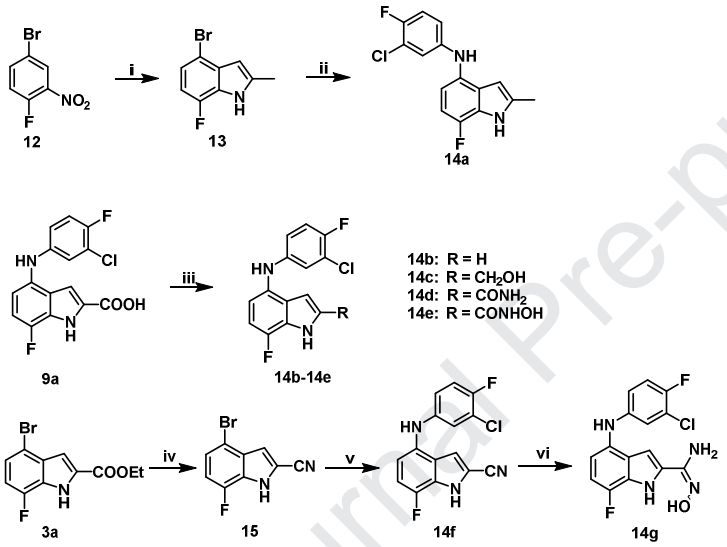

Scheme 3. Reagents and conditions: (i) isopropenyl magnesium bromide, THF, -40 □, 20.6%. (ii) $Pd_2(dba)_3$, DavePhos, K_3PO_4(aq), toluene, 100 □, 28.1%. (iii) Cu, quinoline, MW, 240 □, 46.5%; BH_3·THF, THF, 0 □, 55.7%; EDCI, HOBt, $NH_3.H_2O$ or NH_2OH·HCl, TEA, r.t. 36.8%-48.7%. (iv) NaOH, THF, EtOH, H_2O, 40 □, 99.0%; oxalyl chloride, DMF, DCM, $NH_3.H_2O$, r.t., 99.0%; $POCl_3$, Tol, Ar, reflux, 88.5%. (v) $Pd_2(dba)_3$, X-phos, Cs_2CO_3, 1,4-dioxane, MW, 100 □, 40.9%. (vi) NH_2OH, TEA, EtOH, r.t., 59.0%.

The synthesis of compounds **17a-17f** with different linker groups between indole scaffold and aromatic group was outlined in **Scheme 4**. Compound **16a** with an S atom as the linker group could be constructed by the C-S coupling reaction between compound **3a** and 4-fluoro-3-chlorothiophenol, although the yield is very low. Compound **3a** was coupled with *t*-butyl carbamate, followed by removing the Boc protecting group to form the 4-amino substituted intermediate **19**. Reductive amination of compound **19** with 3-chloro-4-fluorobenzaldehyde resulted in compound **16b**. The reaction of compound **19** with 3-chloro-4-fluorobenzoyl chloride or

3-chloro-4-fluorophenylacetyl chloride led to compounds **16c** and **16e**. Compound **19** was subjected to a nucleophilic addition reaction with 3-chloro-4-fluorophenyl isocyanate to give **16f**. Compound **16d** was prepared by a Pd-catalyzed aminocarbonylation reaction. The 4-Br substituted compound **3a** was carbonylated with carbon monoxide, forming in situ by $CHCl_3$ and CsOH, and then directly reacted with 3-chloro-4-fluoroaniline in a one-pot reaction to produce compound **16d** in 16.9% yield [42]. The target compounds **17a-17f** were obtained by ester hydrolysis of compounds **16a-16f**.

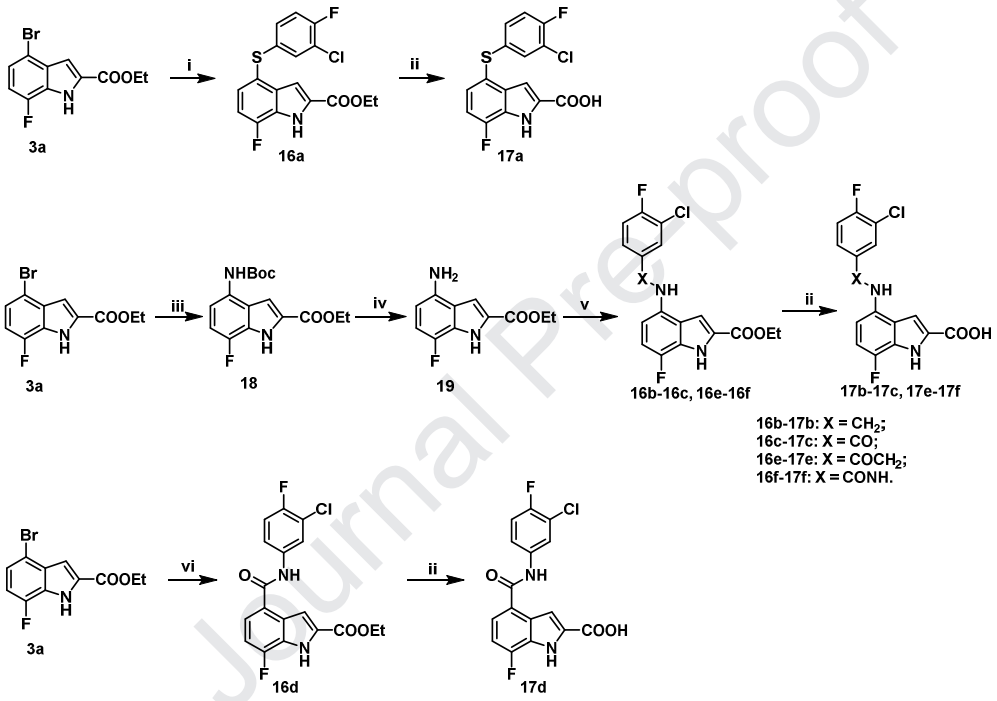

Scheme 4. Reagents and conditions: (i) 3-chloro-4-fluorobenzenethiol, CuI, *N*,*N*-dimethylglycine, Cs_2CO_3, MW, 150 □, 9.7%. (ii) LiOH, THF, EtOH and H_2O, 40 □, 43.4% ~ 97.1%. (iii) NH_2Boc, X-phos, Cs_2CO_3, 1,4-dioxane, 110 □, 70.4%. (iv) CF_3COOH, DCM, r.t., 94.9%. (v) 3-chloro-4-fluorobenzaldehyde, HOAc, $NaBH_4$, DCM, r.t., 66.5%; 3-chloro-4-fluorobenzoic acid, $SOCl_2$, DMF, DCM, TEA, 43.3%; 3-chloro-4-fluorophenylacetic acid, oxalyl chloride, DMF, DCM, TEA, 65%; 3-chloro-4-fluorophenyl isocyanate, DCM, 50.9%. (vi) DPEPhos, $Pd(OAc)_2$, $CHCl_3$, CsOH H_2O, 3-chloro-4-fluoroaniline, Tol, 80 □, 16.9%.

2.2 Inhibitory activities of indole derivatives against IDO1 and TDO enzyme

In order to investigate the structure-activity relationship of indole derivatives, we carried out extensive structure variations on the indole scaffold, including the 6,7-position of the indole skeleton, the indole NH group, 2-carboxyl moiety, and the

substituents on the 4-position. All compounds were evaluated by using recombinant enzyme of IDO1 and TDO and the results were shown in **Tables 1-4**.

2.2.1 Structural modifications on the indole skeleton

By scrutinizing the hits **9a** and **9k**, we speculated that the indole aryl amine frame was a unique structural feature for this class of inhibitors. Therefore, the indole fragment and the aromatic group on the 4-position of indole ring were the focus of the modifications. Initially, the 2-carboxyl-indole ring was kept intact, a variety of substituents were introduced onto the 6- and 7-position of the indole scaffold. As shown in **Table 1**, when the 7-fluorine atom of the hit (**9a**) was removed (**9b**) or replaced with an electron-donating group, such as methyl (**9d**), acetamido (**9h**), or an electron withdrawing group, such as Cl (**9c**), CN (**9f**), NO_2 (**9g**), the inhibitory activities were lost. Only 7-methoxy substituted compound (**9e**, IDO1 IC_{50} = 32.4 μM; TDO IC_{50} = 19.5 μM) retained the inhibitory activity against IDO1 and TDO. Obviously, the modification space of the 7-position is very limited.

The variation of 6-substituents on the inhibitory effects was presented in **Table 1**. The hit (**9k**) with a 6-methyl group had a micromolar level inhibitory activity, and the IC_{50} values for IDO1 and TDO were 35.6 μM and 22.5 μM, respectively. The replacement of methyl group with F (**9i**), Cl (**9j**), OCH_3 (**9l**), CN (**9m**), or NO_2 (**9n**) substituent led to the loss of potency, while the acetamido (**9o**) or ethylamino group (**9p**) was incorporated onto the 6-position, the compounds had strong inhibitory activities against both enzymes. The IC_{50} values for IDO1 of 8.40 μM and 1.75 μM, respectively, and the inhibitory activity against TDO was comparable to that of IDO1, showing IC_{50} values of 8.48 μM and 3.53 μM, respectively. The 6-acetamido substituent or 6-ethylamine group was favorable for increasing the inhibitory activity. It was assumed that these substituents might contribute to the binding of IDO1 or TDO through hydrogen bonds. Among this series of compounds, the 6-ethylamino substituted compound (**9p**) showed the strongest inhibitory activity, which was 23 times more active than the hit compound (**9a**). However, due to the high electron density nature of this indole ring, compound (**9p**) was readily oxidized and unstable.

Therefore, in the subsequent structural optimization of the substituents on the 4-position of the indole scaffold, we selected the 6-acetamido substituted compound (**9o**) as a new lead compound for further SAR exploration.

The methylation of indole nitrogen was conducted on the hits **9a** and **9k** as well. And none of the two compounds (**9q** and **9r**) had inhibitory activity. Furthermore, we also tentatively replaced the indole ring with a benzothiophene fragment (**9s**), which had no inhibitory activity against IDO1. These results suggested that the NH in the indole ring was important for the binding activity, presumably because NH was involved in a hydrogen bonding and/or a steric hindrance was generated by the introduction of the methyl group.

Table 1. Enzyme inhibitory activities for 6- or 7-substituted or 1-substituted indole-2-carboxylic acid derivatives 9a-9s

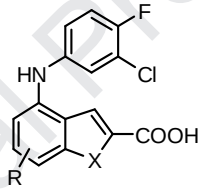

Compound	R	X	IC_{50} (μM)±SD	
			IDO1	TDO
9a	7-F	NH	40.7±3.03	99.2±51.5
9b	H	NH	>100	N.D. [a]
9c	7-Cl	NH	>100	N.D.
9d	7-CH_3	NH	>100	N.D.
9e	7-OCH_3	NH	32.4±4.95	19.5±0.47
9f	7-CN	NH	>100	N.D.
9g	7-NO_2	NH	>100	N.D.
9h	7-$NHCOCH_3$	NH	>100	N.D.
9i	6-F	NH	>100	N.D.
9j	6-Cl	NH	>100	N.D.
9k	6-CH_3	NH	35.6±3.93	22.5±3.30
9l	6-OCH_3	NH	>100	N.D.
9m	6-CN	NH	>100	>100
9n	6-NO_2	NH	>100	>100
9o	6-$NHCOCH_3$	NH	8.40±1.70	8.48±0.40
9p	6-NHC_2H_5	NH	1.75±0.12	3.53±0.83
9q	7-F	NCH_3	>100	N.D.

9r	6-CH_3	NCH_3	>100	N.D.
9s	6-$NHCOCH_3$	S	>100	N.D.
Epacadostat	-	-	0.058±0.012	-
Navoximod	-	-	0.075±0.017	0.80±0.051

[a] not detected.

The SAR on the 2-position of the indole scaffold was investigated preliminarily with an attempt to displace carboxyl group to improve the drug-like property. However, as shown in **Table 2**, the results demonstrated that the 2-carboxyl group played a critical role in the binding. The replacement of the carboxyl group with a methyl (**14a**), hydroxymethyl (**14c**) or cyano group (**14f**), or removal of the carboxyl group (**14b**) resulted in loss of inhibition. In particular, the close bioisosteric group of carboxyl moiety, including the carbamoyl (**14d**), hydroxamic acid (**14e**), and hydroxycarbamimidoyl group (**14g**), was grafted onto the 2-position, the inhibition disappeared as well. We conjectured that the carboxyl anion might act as an electron donor to cooperate with the iron ion in the heme of IDO1. After incubation compound **9a** with IDO1, the UV spectrum was measured and the wavelength did not show the red-shift [43], suggesting that compound **9a** did not cooperate with the iron ion in IDO1. Therefore, we speculated that the carboxyl group was supposed to bind with the key amino acids within IDO1/TDO via electrostatic interactions.

Table 2. Enzyme inhibitory activities for 2-substituted indole derivatives 14a-14g

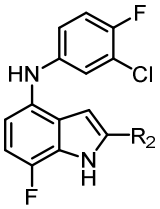

Compound	R_2	IC_{50} (μM)	
		IDO1	TDO
9a	COOH	40.7±3.03	99.2±51.5
14a	CH_3	>100	N.D.[a]
14b	H	>100	N.D.
14c	CH_2OH	>100	N.D.
14d		>100	N.D.

14e	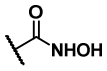	>100	N.D.
14f	CN	>100	N.D.
14g		>100	N.D.
Epacadostat	-	0.058±0.012	-
Navoximod	-	0.075±0.017	0.80±0.051

[a] not detected.

The NH group on the 4-position of indole ring could be regarded as a linker between the indole scaffold and the aromatic group. The influence of this linker on the inhibition was also evaluated. As shown in **Table 3**, one-atom linker such as S atom (**17a**), two-atom linker such as aminomethylene (**17b**), carbamoyl (**17c**), formamido (**17d**), or three-atom linker such as $NHCOCH_2$ (**17e**) or urea group (**17f**) was utilized and all of the resultant compounds showed no inhibition against IDO1. These results indicated that the linker NH was an important pharmacophore fragment. It is assumed that the NH group not only provides a suitable distance between the indole ring and the aromatic moiety, but also might serve as a hydrogen bond donor to contribute to the binding.

Table 3. Enzyme inhibitory activities for 4-substituted indole-2-carboxylic acid compounds 17a-17f.

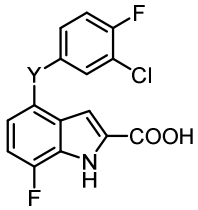

Compound	Y	IC_{50} (μM)	
		IDO1	TDO
9a	NH	40.7±3.03	99.2±51.5
17a	S	>100	N.D.[a]
17b	-$NHCH_2$-	>100	N.D.
17c	-NHCO-	>100	N.D.
17d	-CONH-	>100	N.D.
17e	-$NHCOCH_2$-	>100	N.D.
17f	-NHCONH-	>100	N.D.

Epacadostat	-	0.058±0.012	-
Navoximod	-	0.075±0.017	0.80±0.051

[a] not detected.

Taken together, the efforts on the modifications of indole ring demonstrated that 2-carboxyl indole ring and 4-amino linker were the essential structure moiety for producing inhibition against IDO1 and TDO. Grafting an acetamido or ethylamino group was favorable for the binding and giving rise to micromolar inhibitors, although only very limited substituents were allowed to incorporate onto the 6- and 7-position of the indole ring. Therefore, we selected two representative indole scaffolds, one is 7-fluoro-2-carboxyl-indole and the other is 6-acetamido-2-carboxyl-indole, as the templates for further SAR explorations on the aromatic moiety of compounds **9a** and **9o**.

2.2.2 Structural modifications on the aryl ring

The variation of aromatic group of compound **9a** was performed and the results were presented in **Table 4**. When the 4'-position was a fluorine atom, the 3'-position was substituted by Cl (**9a**), Br (**9a-2**), OCH_3 (**9a-3**) or OCF_3 (**9a-4**), respectively, the obtained compounds had moderate inhibitory activities, while a fluorine atom (**9a-1**) or cyano group (**9a-5**) was placed, loss of inhibition was observed. When the 3'-Cl in the hit **9a** was maintained, and the 4'-F was replaced by various groups, such as Cl, OCH_3, OCF_3 or CF_3, none of them (**9a-6~9a-9**) produced inhibitory effects on IDO1. These results indicated that a steric bulky hydrophobic group was allowed on the 3'-position while there is a limited space for the substituents on the 4'-position. The F atom on the 4'-position of the benzene ring was beneficial to the inhibitory activity.

Except for the 3',4'-disubstituted phenyl groups, other substituted benzene rings were explored as well. The derivatives bearing 3'-methoxy-5'-trifluoromethyl (**9a-10**), 3'-methoxy-5'-chloro (**9a-11**) or 2'-carboxy-5'-methoxy (**9a-13**) substituent had no inhibitory activity. Compounds with 2'-fluoro-5'-bromo (**9a-12**, IDO1 IC_{50} = 28.1 μM, TDO IC_{50} = 41.4 μM) or 3',4',5'-trimethoxyl (**9a-14,** IDO1 IC_{50} = 22.2 μM; TDO IC_{50} = 23.3 μM) substituent had moderate inhibitory activity. We also examined the

inhibitory effect of the indoleamine and its derivatives substituted for the 3'-chloro-4'-fluoro-benzene amine. When the indoleamine (**9a-15**) or 7'-F-indoleamine (**9a-16**) was utilized, the compounds showed no inhibitory activity. Surprisingly, compound **9a-17** bearing 7'-fluoro-2'-carboxy-indoleamine at the 4-position of the indole scaffold showed a pronounced potency against IDO1 and TDO, the IC_{50} values are 2.72 μM and 3.48 μM, respectively, which is 15 and 28.5 times higher than that of hit compound **9a**. Compound **9a-17** had the strongest inhibitory activity against IDO1 among the 7-fluoro-indole-2-carboxylic acid series of compounds. Overall, both the substitution pattern of the benzene ring and the properties of the substituents have impacts on the inhibitory activity, and further modifications on this moiety might provide chance to improve the potency.

Table 4. Enzyme inhibitory activities for 4-arylamino-7-fluoro-indole-2-carboxylic acid derivatives 9a-1~9a-17

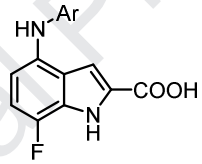

Compound	Ar	IC_{50} (μM)	
		IDO1	TDO
9a	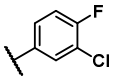	40.7±3.03	99.2±51.5
9a-1	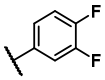	>100	N.D.[a]
9a-2	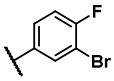	9.93±0.85	10.5±0.06
9a-3	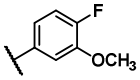	54.4±15.7	31.4±1.44
9a-4	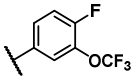	16.3±2.33	16.5±1.96
9a-5	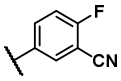	>100	N.D.
9a-6	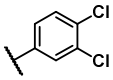	>100	N.D.
9a-7	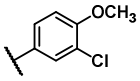	>100	N.D.
9a-8	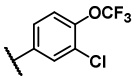	>100	N.D.

9a-9	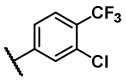	>100	N.D.
9a-10	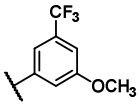	>100	N.D.
9a-11	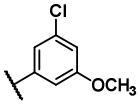	>100	N.D.
9a-12	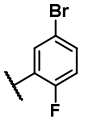	28.1±3.72	41.4±4.25
9a-13	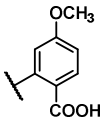	>100	N.D.
9a-14	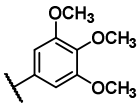	22.2±2.34	23.3±0.46
9a-15	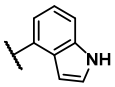	>100	N.D.
9a-16	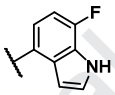	>100	N.D.
9a-17	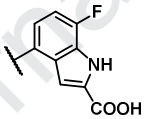	2.72±0.67	3.48±0.22
Epacadostat	-	0.058±0.012	-
Navoximod	-	0.075±0.017	0.80±0.051

[a] not detected.

The SAR investigation based on the template 6-acetamido-indole-2-carboxylic acid was also carried out and the inhibitory activities were listed in **Table 5**. According to the previous SAR results, the fluoro atom was kept on the 4'-position of the benzene ring, and a variety of substituents were incorporated onto the 3'-position to explore the SAR of this series of derivatives first. Satisfyingly, grafting a fluoro atom and various hydrophobic groups of different sizes (**9o-1 ~ 9o-13**), all compounds produced noticeable inhibition against IDO1 and TDO, the IC_{50} value ranged from 1.17 μM to 10.0 μM for IDO1 and 1.44 μM to 9.63 μM for TDO. Compound **9o-1** with a 3', 4'-difluoro phenyl group exhibited marked inhibition against both enzymes (IDO1 IC_{50} = 1.17 μM, TDO IC_{50} = 1.55 μM), and it is the most potent dual inhibitor

in this class of indole inhibitors. Among the alkyloxyl substituted derivatives (**9o-2 ~ 9o-8**), compounds with a relatively smaller size group, such as methoxyl (**9o-2**), ethoxyl (**9o-3**), propoxyl (**9o-4**) and trifluoromethoxyl (**9o-5**), showed strong inhibition against IDO1 with IC_{50} values at the low micromolar level, and potent inhibition against TDO as well. In contrast, the placement of somewhat larger groups, such as isopropoxyl (**9o-6**), cyclopropylmethoxyl (**9o-7**), or trifluoroethoxyl (**9o-8**) moiety would result in a slightly decrease in potency. The incorporation of even more bulky substituents, such as phenoxyl (**9o-9**) and benzyloxyl (**9o-10**) moiety led to more reduction in inhibition. In comparison with that of compound **9o-1**, the inhibition of compound **9o-10** decreased by 8.5-fold against IDO1 and 3.4-fold against TDO, respectively. These results demonstrated that the inhibitory activity decreased with increasing the size of the 3'-substituent on the benzene ring.

Table 5. Enzyme inhibitory activities for 4-arylamine-6-acetamido-indole-2-carboxylic acid derivatives 9o-1 ~ 9o-24

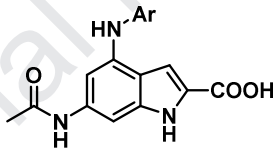

Compound	Ar	IC_{50} (μM)	
		IDO1	TDO
9o	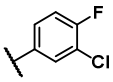	8.40±1.70	8.48±0.40
9o-1	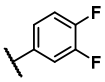	1.17±0.15	1.55±0.25
9o-2	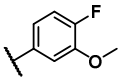	1.23±0.33	2.49±0.16
9o-3	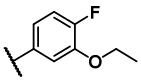	2.20±0.01	5.13±0.68
9o-4	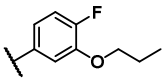	1.48±0.15	4.46±0.08
9o-5	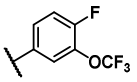	1.37±0.18	3.62±0.21
9o-6	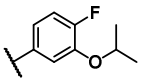	3.09±0.35	6.46±1.59
9o-7	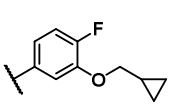	3.11±0.35	4.09±0.98

9o-8	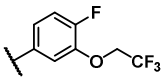	4.62±0.83	9.63±0.63
9o-9	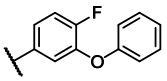	5.83±1.53	1.44±0.13
9o-10	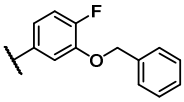	10.0±1.07	5.24±0.94
9o-11	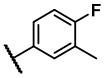	1.83±0.18	1.70±0.49
9o-12	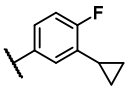	2.95±0.38	5.45±0.18
9o-13	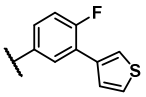	3.89±0.31	2.53±0.40
9o-14	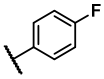	5.28±1.01	7.69±0.11
9o-15	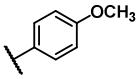	1.71±0.53	3.01±0.01
9o-16	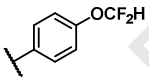	3.18±0.27	5.50±0.31
9o-17	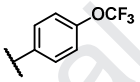	23.7±6.89	5.71±0.78
9o-18	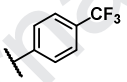	55.5±39.4	23.2±2.14
9o-19	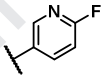	38.5±2.65	46.1±6.24
9o-20	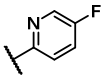	10.8±0.83	11.7±0.91
9o-21	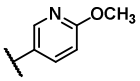	3.41±0.39	3.62±0.31
9o-22	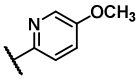	4.73±0.49	5.27±2.55
9o-23	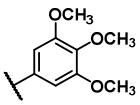	3.18±0.56	7.12±0.27
9o-24	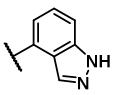	7.52±2.35	6.78±0.05
Epacadostat	-	0.058±0.012	-
Navoximod	-	0.075±0.017	0.80±0.051

As to the alkyl substituted derivatives, the similar trend was observed. Compound **9o-11** (IDO1 IC_{50} = 1.83 μM; TDO IC_{50} = 1.70 μM) with a methyl group

was more potent than compound **9o-12** (IDO1 IC_{50} = 2.95 μM; TDO IC_{50} = 5.45 μM) with a cyclopropyl substituent. The thienyl substituted derivative **9o-13** had similar potency to compound **9o-12**. These results demonstrated that a small hydrophobic group such as F, OCH_3 and CH_3 on the 3'-position was favorable for the inhibition.

The compounds with mono-substituted benzene ring or pyridine ring (**9o-14 ~ 9o-22**) were also evaluated as shown in **Table 5**. The 4'-fluoro substituted derivative (**9o-14**) displayed comparable activity to compound **9o.** Compound **9o-15** (IDO1 IC_{50} = 1.71 μM; TDO IC_{50} = 3.01 μM) with a methoxyl group produced an improved activity compared with compounds **9o** and **9o-14.** Especially, when the substituents OCF_2H or OCF_3 was brought in, the inhibition against IDO1 would be inflicted significantly (IDO1 inhibition, 4'-OCH_3 > 4'-OCF_2H > 4'-OCF_3). These data indicated that the oxygen atom on the 4'-position played an important role and it might serve as an H-bond acceptor, as the ability of forming H-bond decreased with the fluoro atom increasing. In addition, compound **9o-18** (IDO1 IC_{50} = 55.5 μM; TDO IC_{50} = 23.2 μM) with a trifluoromethyl group showed pronounced reduction against both enzymes. This result further supported that an H-bond acceptor such as F or O atom on the 4'-position was critical for the binding.

In comparison with compounds **9o-14** and **9o-15,** the pyridine derivatives (**9o-19 ~ 9o-22**) showed reduction in potency, partly due to the decreased H-bond forming capability of the fluoro atom and the methoxyl group, presumably.

In this series, we also prepared compound **9o-23** with a trimethoxyl substituted benzene ring and compound **9o-24** bearing an indazole fragment. Both of them displayed micromolar inhibition against the two enzymes. This result further suggested that various aromatic groups could be tolerated at the 4-position of the indole scaffold.

Generally, 6-acetamido-indole-2-carboxylic acid derivatives are more potent than the 7-fluoro-substituted series, as exemplified by compounds **9o-1** (IDO1 IC_{50} = 1.17 μM; TDO IC_{50} = 1.55 μM) and **9o-2** (IDO1 IC_{50} = 1.23 μM; TDO IC_{50} = 2.49

μM), which possess remarkable potency against both enzymes, while the counterpart of 7-fluoro-substituted derivatives (compounds **9a-1** and **9a-3**) showed very weak inhibition with $IC_{50} > 10^{-5}$ M. In addition, the aromatic moiety on the 4-position of 6-acetamido substituted series was allowed to be varied to a greater extent, and thus providing more opportunities for further improving potency.

2.3 The structure confirmation and activity evaluation of the oxidation product of compound 9p

We accidentally found that compound **9p** was unstable and easily oxidized. The oxidation product was isolated and identified by ^{1}H-NMR and MS, which could be *p*-benzoquinone **9p-O**. In order to confirm the structure of compound **9p-O**, a targeted synthesis was designed as shown in **Figure 2**. Compound **8p** was oxidized with mCPBA to yield compound **8p-O**, which was confirmed to be a *p*-benzoquinone by X-ray single crystal diffraction (**Figure 2**). The ester hydrolysis of compound **8p-O** gave rise to compound **9p-O**. Surprisingly, compound **9p-O** exhibited strong inhibitory activity against IDO1 with IC_{50} value of 18 nM and TDO with IC_{50} value of 25 nM, respectively.

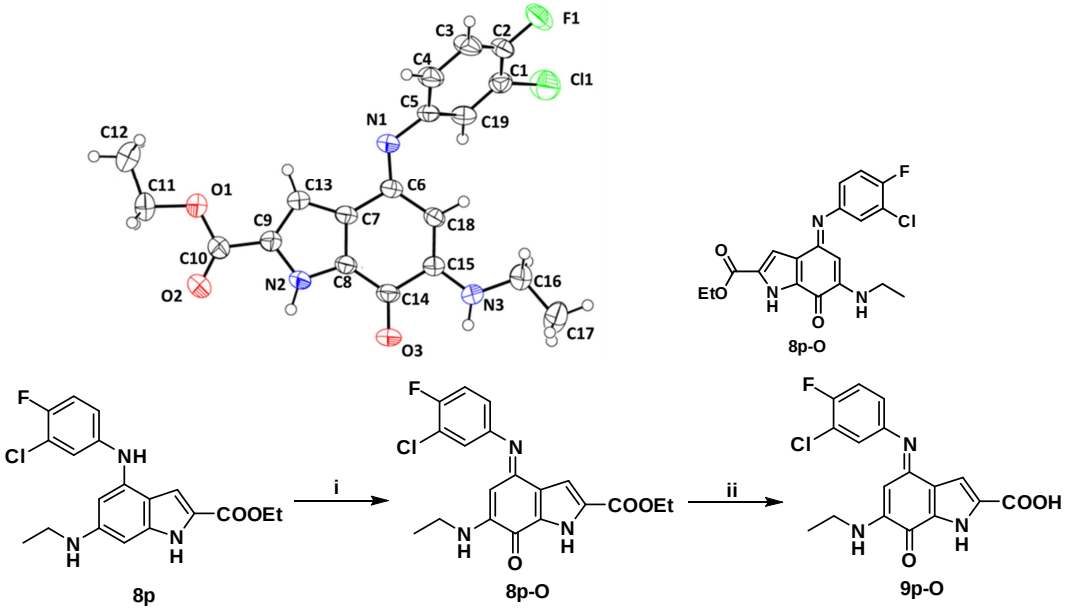

IDO1 IC_{50} = 18 nM

TDO IC_{50} = 25 nM

Reagents and conditions: (i) m-CPBA, 0 □, DCM, 81%. (ii) LiOH, r.t., THF, H_2O, 59.5%

Figure 2. The crystal structure of compound **8p-O** and the preparation of oxidation product **9p-O.**

2.4 Predicted binding modes of compound 9o to IDO1 and TDO

In order to explore the binding mode of this class of compounds, compound **9o** which served as a template and lead structure of the 6-acetamido-indole-2-carboxylic acid series was tentatively selected and docked into the crystal structures of IDO1 (5WMU) [44] and TDO (5TIA) [8], respectively, by using CDOCKER protocol integrated in Accelrys Discovery Studio [45]. And then molecular dynamics simulation was performed with Amber16 package [46] to further optimize the binding pose of compond **9o** within the binding pocket of each enzyme (the results of MD simulation shown in supplementary information S1). As shown in **Figure 3**, compound **9o** occupies the pocket on the top of heme molecule in both IDO1 and TDO, the overall orientations are alike. However, the precise binding poses are somewhat different. In IDO1 (**Figure 3A** and **3B**), the NH and carbonyl oxygen on 6-acetamido group form hydrogen bonds with key amino acid residues Gly262 and Cys129, respectively. The 2-carboxylate group on the indole scaffold creates H-bonds with key amino acid residues Tyr126 and Ser167 as well. These hydrogen bonding interactions are supposed to make critical contributions to the binding since the acetamido and carboxyl moieties are essential pharmacorphore groups as SAR demonstrated. The indole ring forms a T-shape π-π interaction with Phe163, which is also an important feature for known IDO1 inhibitors [27, 47]. The 4'-fluoro-3'-chloro-phenyl group on the 4-position extends into a subpocket close to Arg231, and the 4'-F can build a hydrogen bond with the key amino acid Arg231. This is also consistant with the SAR that an H-bond acceptor on the 4'-position is benefical to the inhibitory potency.

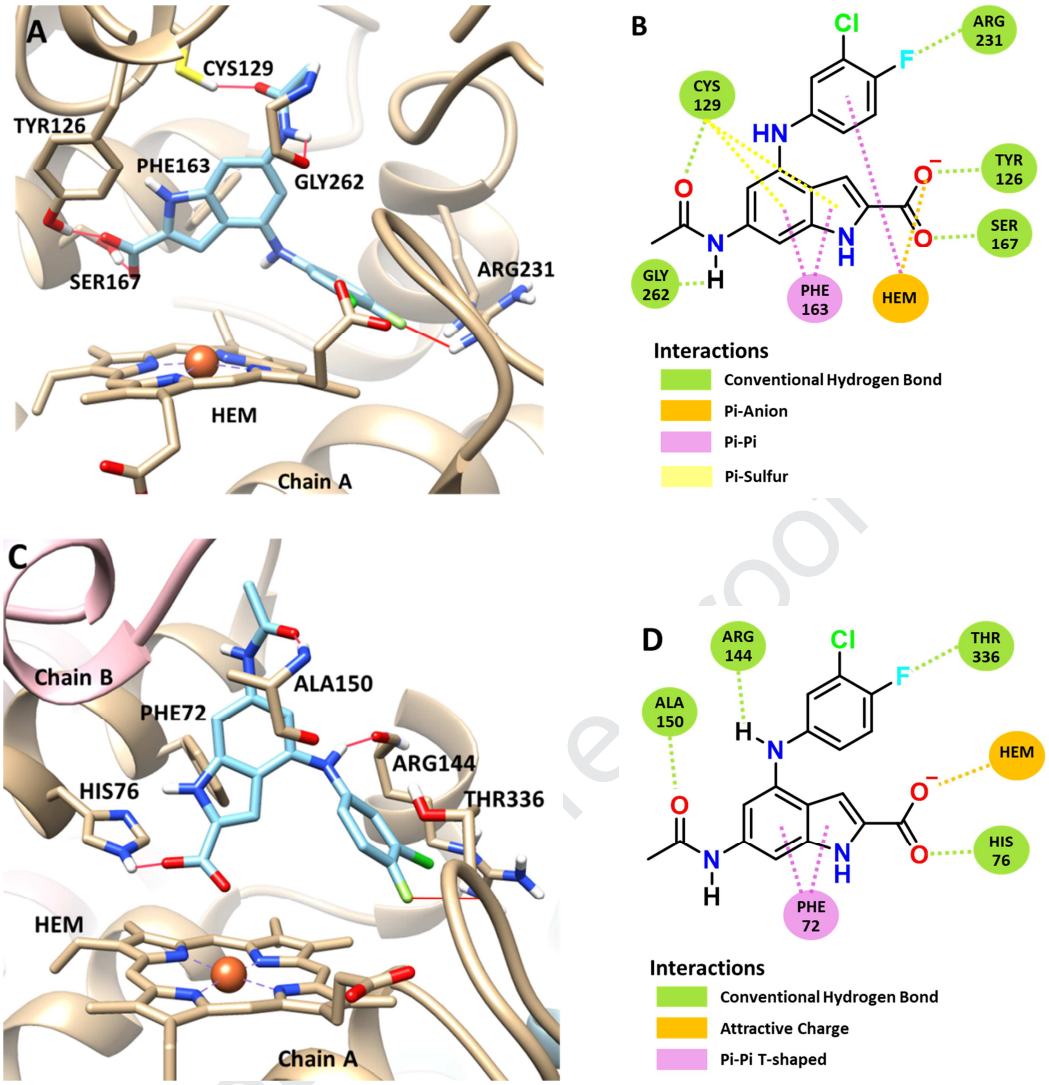

Figure 3. Predicted binding modes of compound **9o** to IDO1 (A and B) and TDO (C and D) using CDOCKER and dynamics simulation. (A, C): The binding mode of compound **9o** to IDO1(5WMU, A) and TDO (5TIA, C), the enzyme is shown in gold, compound **9o** is shown as sticks with sky blue carbon atoms. The residues that interact with compound **9o** are shown as sticks with gold carbon atoms, and hydrogen bonds are indicated by red lines. The images were generated by using Chimera 1.12. (B, D): The schematic 2D diagram of the key interactions in between compound **9o** with IDO1 (5WMU, B) and TDO (5TIA, D), respectively.

Compared with IDO1, one of the key differences within the binding pocket is that an His76 is situated on the top of heme in TDO and the corresponding amino acid is Ser167 in IDO1 (**Figure 3C** and **3D**). Due to the presence of a large side chain of His76, the carboxyl group of compound **9o** moves slightly toward the heme molecule in TDO, resulting in a different binding pose within the cavity of TDO. The 2-COOH not only constructs an H-bond with His76, but also can build an electrostatic interaction with the ferrous ion of the heme. The $NHCOCH_3$ group can interact with

Ala150 via a hydrogen bond. The indole ring establishes hydrophobic interactions with Ala150 and Phe72. These binding features of compound **9o** suggested that 6-acetamido-2-carboxyl-indole scaffold played a crucial role in TDO binding as well. It is noted that the NH group on the 4-position of the indole ring forms an H-bond with the carbonyl oxygen of Arg144 in TDO, while it has no interaction in IDO1. The 4'-F of benzene ring forms a hydrogen bond with the key amino acid Thr336. This also demonstrated that an appropriate H-bond acceptor such as F or OCH_3 group on the 4'-position could contribute to the binding affinity to some extent. Taken together, the binding modes indicated that the 6-acetamido-2-carboxyl-indole ring and the 4'-fluoro-substituted benzene ring are characteristic moieties of this class of dual inhibitors, which make essential contributions to the binding to both enzymes, although the binding poses of compound **9o** and the involved key amino acids within the pocket are somewhat different.

2.5 Cellular IDO1/TDO inhibitory activities of indole-2-carboxylic acid derivatives

As the series of compounds bearing the 6-acetamido-indole-2-carboxylic acid scaffold presented potent enzymatic inhibition, most of them were further tested for their cellular IDO1 and TDO inhibitory activity using A172 cells. IFNγ was used to induce the overexpression of IDO1 and TDO in A172 cells. The inhibitory activity was determined by measuring the amount of the kynurenine released from the cells [48, 49]. The results (see supplementary information S2) showed that compound **9o-23** was the most potent inhibitor, which had an inhibition rate of 77.7% at the concentration of 100 μM and 55.9% at 50 μM concentration, respectively.

2.6 Effects of indole-2-carboxylic acid derivatives on T cell proliferation

Both IDO1 and TDO could contribute to the tumor progression through its capability to block T lymphocyte proliferation by consuming Trp locally. Thus, to determine whether this class of dual inhibitors could enhance the T cell proliferation which was stimulated by LLC cells, we performed T cell proliferation assay using compound **9o-23** with the cellular inhibitory activity [17]. As shown in **Figure 4**,

Compound **9o-23** could increase the proliferation of T cells at a concentration of 10 μM noticeably, although it much less potent than Navoximod. The results demonstrated that compound **9o-23** could reverse the suppression of T lymphocyte caused by IDO1 and TDO.

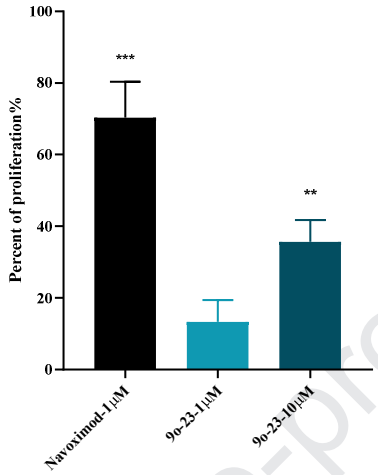

Figure 4. Compound **9o-23** increased the proliferation of T cells stimulated with LLC tumor cells. Each bar of the graph indicates the mean of three replicate wells with standard error of the mean. (*) $P < 0.05$, (**) $P < 0.01$, (***) $P < 0.001$ compare to vehicle control.

2.7 Antitumor activity evaluation of compound 9o-23

As compound **9o-23** exhibited potent IDO1/TDO inhibition on both enzymatic and cellular assay, along with its capability to induce T cell proliferation, it was selected for further *in vivo* antitumor evaluation. The antitumor activity of compound **9o-23** against mouse B16F10 melanoma was carried out on a mouse subcutaneous xenograft model. After consecutive administration of 19 days, the tumor growth inhibition was observed (Figure 5, A). The inhibition was 43.2% at the dose of 50 mg/kg, and 44.7% at the dose of 100 mg/kg, respectively. In addition, the body weight of the treated mice had no significant loss compared with the control group. These data further suggested that this series of novel dual inhibitors could serve as promising lead structure for developing highly potent and drug-like dual inhibitors to be useful for the treatment of cancer.

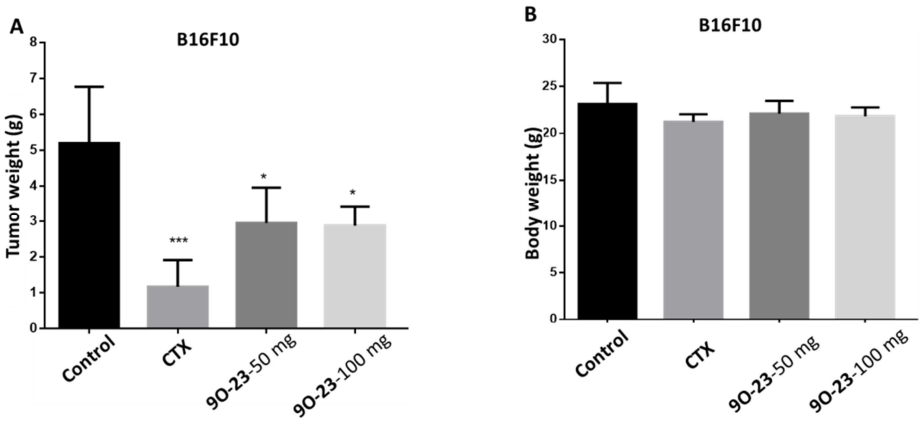

Figure 5. In vivo anti-tumor activity of **9o-23** in B16F10 xenograft mice. (**A**) Tumors weights of each group after 19 days of treatment. The control group mice bearing B16F10 xenografts were dosed orally with vehicle (0.5% Sodium salt of Caboxymethyl Cellulose, CMC-Na); the CTX (Cyclophosphamide) group were administered CTX intraperitoneally at the dose of 100 mg/kg; the treated group were administered **9o-23** orally at the dose of 50 mg/kg or 100 mg/kg. * $p < 0.05$ and *** $p < 0.001$ versus vehicle. (**B**) The body weight of each group after the treatment. There is no obvious body weight difference among all of the groups.

3. Conclusion

Based on the hits **9a** and **9k** identified by a random screening, a variety of indole-2-carboxylic acid derivatives were synthesized and their inhibitory activity against IDO1 and TDO were evaluated. The structure-activity relationships were investigated extensively and resulted in a new class of dual inhibitors with a 6-acetamido-indole-2-carboxylic acid scaffold, as exemplified by compounds **9o** and **9o-1 ~ 9o-24**. The binding modes of compound **9o** gave some insights for rationalizing the SARs. The scaffold situated in a relatively restricted subpocket on the top of the heme and the space of structural modifications was very limited. In contrast, the aromatic moiety on the 4-position extended into an area around a loop and Arg231 (Arg144 in TDO), which possessed some extent flexibility and provided an opportunity for structural optimization to improve the potency and diversity, as the SAR results demonstrated.

In addition, a new para-benzoquinone derivative compound **9p-O** was identified, which displayed strong inhibitory activity with IC_{50} value at the double digit nanomolar level against both IDO1 and TDO, respectively.

In summary, novel IDO1 and TDO dual inhibitors were disclosed and the results obtained in this work will guide further structural optimizations for the development of diversified new chemical entities with improved potency.

4. Experimental section

4.1 Chemical Synthesis General

^{1}H NMR spectra were recorded with a Varian Mercury 400 or 500 spectrometer using tetramethylsilane (TMS) as the internal standard in Acetone d_6, DMSO d_6 or $CDCl_3$. High preparation mass spectra (HRMS) were recorded on an Agilent Technologies LC/MSD TOF spectrometer. Melting points were measured on a Yanaco micro melting point apparatus. All chemicals and solvents used were of reagent grade without further purification or dried before used. All the reactions were monitored by thin-layer chromatography (TLC) under a UV lamp at 254 nm. Column chromatography separations were performed with silica gel (200-300 mesh).

4.2. General procedure for preparation of 1*H*-indole-2-carboxylic acids (9a-9s, 9a-1~9a-17, 9o-1~9o-24)

Method 1: To a solution of compound **8** in THF/EtOH (1:1) was added 1.0 M NaOH solution (5 eq) dropwise and stirred at room temperature overnight. The solvent was evaporated in vacuo and the residue was acidified with 1N HCl. After filtration, the title compound was obtained. Compounds **9a-9e**, **9g-9o**, **9q-9s**, **9a-2**~**9a-4**, **9a-6**, **9a-12**~**9a-14**, **9a-17**, **9o-2**, **9o-3**, **9o-5**, **9o-11**~**9o-13**, **9o-23** were prepared with method 1.

Method 2: To a solution of compound **8** in THF/EtOH (1:1) was added 1.0 M LiOH solution (5 eq) dropwise and stirred at 40 □ until the ester group was completely hydrolyzed. The solvent was evaporated in vacuo and the residue was acidified with 1N HCl. After filtration, the title compound was obtained. Compounds **9f**, **9a-1**, **9a-5**, **9a-7**~**9a-11**, **9o-1**, **9o-4**, **9o-6**~**9o-10**, **9o-14**~**9o-22**, **9o-24** were prepared with method 2.

Method 3: To a solution of compound **8** in EtOH was added 1.0 M Na_2CO_3 solution (5 eq) and stirred at refluxing temperature until the ester group was completely hydrolyzed. The solvent was evaporated in vacuo and the residue was acidified with 1N HCl. After filtration, the title compound was obtained. Compounds **9p**, **9a-15**, **9a-16** were prepared with method 3.

4.2.1. 4-((3-Chloro-4-fluorophenyl)amino)-7-fluoro-1*H*-indole-2-carboxylic acid (9a): copper green solid, yield: 99.0%, mp: 135-137 □, ^{1}H-NMR (400 MHz, DMSO-d_6) δ (ppm): 13.06 (brs, 1H), 12.24 (s, 1H), 8.30 (s, 1H), 7.27-7.24 (m, 2H), 7.17 (dd, J_1 = 6.5 Hz, J_2 = 2.5 Hz, 1H), 7.05 (ddd, J_1 = 9.0 Hz, J_2 = 4.0 Hz, J_3 = 3.0 Hz, 1H), 6.97 (dd, J_1 = 10.5 Hz, J_2 = 8.0 Hz, 1H), 6.73 (dd, J_1 = 8.5 Hz, J_2 = 3.5 Hz, 1H); HRMS (ESI): *m/z*, Calcd. for $C_{15}H_{10}O_2N_2ClF_2$ $[M+H]^+$: 323.0393, Found 323.0393.

4.2.2. 4-((3-Chloro-4-fluorophenyl)amino)-1*H*-indole-2-carboxylic acid (9b): copper green solid, yield: 94.0%, mp: 182-183 □, ^{1}H-NMR (400 MHz, Acetone-d_6) δ (ppm): 10.87 (brs, 1H), 7.34 (s, 1H), 7.31 (d, J = 5.6 Hz, 1H), 7.24-7.14 (m, 4H), 6.92 (d, J = 7.2 Hz, 1H); HRMS (ESI): *m/z*, Calcd. for $C_{15}H_{11}O_2N_2ClF$ $[M+H]^+$: 305.0488, Found 305.0495.

4.2.3. 7-Chloro-4-((3-chloro-4-fluorophenyl)amino)-1*H*-indole-2-carboxylic acid (9c): brown solid, yield: 98.0%, mp: 237-239 □, ^{1}H-NMR (400 MHz, DMSO-d_6) δ (ppm): 13.02 (brs, 1H), 11.87 (s, 1H), 8.45 (s, 1H), 7.41 (s, 1H), 7.33-7.27 (m, 2H), 7.18-7.14 (m, 2H), 6.79 (d, J = 8.4 Hz, 1H); HRMS (ESI): *m/z*, Calcd. for $C_{15}H_{10}O_2N_2Cl_2F$ $[M+H]^+$: 339.0098, Found 339.0097.

4.2.4. 4-((3-Chloro-4-fluorophenyl)amino)-7-methyl-1*H*-indole-2-carboxylic acid (9d): white solid, yield: 95.0%, mp: 224-226 □, ^{1}H-NMR (400 MHz, DMSO-d_6) δ (ppm): 12.82 (s, 1H), 11.58 (s, 1H), 8.21 (s, 1H), 7.24 (t, J = 8.8 Hz, 2H), 7.15 (dd, J_1 = 6.0 Hz, J_2 = 1.6 Hz, 1H), 7.05-7.03 (m, 1H), 6.92 (d, J = 7.2 Hz, 1H), 6.75 (d, J = 7.6 Hz, 1H), 2.44 (s, 3H); HRMS (ESI): *m/z*, Calcd. for $C_{16}H_{13}O_2N_2ClF$ $[M+H]^+$:

319.0644, Found 319.0645.

4.2.5. 4-((3-Chloro-4-fluorophenyl)amino)-7-methoxy-1*H*-indole-2-carboxylic acid (9e): brownish green solid, yield: 99.0%, mp: 193-195 □, ^{1}H-NMR (400 MHz, DMSO-d_6) δ (ppm): 11.71 (s, 1H), 8.05 (s, 1H), 7.20 (t, J = 8.8 Hz, 1H), 7.10 (s, 1H), 7.01 (d, J = 5.2 Hz, 1H), 6.92-6.89 (m, 1H), 6.77 (d, J = 8.0 Hz, 1H), 6.71 (d, J = 8.0 Hz, 1H), 3.87 (s, 3H); HRMS (ESI): m/z, Calcd for $C_{16}H_{13}O_3N_2ClF$ $[M+H]^+$: 335.0593, Found 335.0595.

4.2.6. 4-((3-Chloro-4-fluorophenyl)amino)-7-cyano-1*H*-indole-2-carboxylic acid (9f): yellow solid, yield: 97.7%, mp: >250 □, ^{1}H-NMR (400 MHz, DMSO-d_6) δ (ppm): 13.07 (brs, 1H), 12.50 (s, 1H), 9.03 (s, 1H), 7.57-7.55 (m, 2H), 7.47 (dd, J_1 = 6.4 Hz, J_2 = 2.4 Hz, 1H), 7.43 (t, J = 8.8 Hz, 1H), 7.34-7.30 (m, 1H), 6.75 (d, J = 8.0 Hz, 1H); HRMS (ESI): m/z, Calcd for $C_{16}H_{10}O_2N_3ClF$ $[M+H]^+$: 330.0440, Found 330.0426.

4.2.7. 4-((3-Chloro-4-fluorophenyl)amino)-7-nitro-1*H*-indole-2-carboxylic acid (9g): red-brown solid, yield: 97.0%, mp: 242-244 □, ^{1}H-NMR (400 MHz, DMSO-d_6) δ (ppm): 10.80 (s, 1H), 9.71 (s, 1H), 8.14 (d, J = 9.2 Hz, 1H), 7.74 (s, 1H), 7.60 (dd, J_1 = 6.4 Hz, J_2 = 2.4 Hz, 1H), 7.50 (t, J = 8.8 Hz, 1H), 7.43-7.40 (m, 1H), 6.72 (d, J = 9.2 Hz, 1H); HRMS (ESI): m/z, Calcd for $C_{15}H_{10}O_4N_3ClF$ $[M+H]^+$: 350.0338, Found 350.0341.

4.2.8. 7-Acetamido-4-((3-chloro-4-fluorophenyl)amino)-1*H*-indole-2-carboxylic acid (9h): brown solid, yield: 79.1%, mp: 177-179 □, ^{1}H-NMR (400 MHz, DMSO-d_6) δ (ppm): 13.07 (brs, 1H), 11.55 (s, 1H), 9.67 (s, 1H), 8.25 (s, 1H), 7.72 (d, J = 8.0 Hz, 1H), 7.25 (t, J = 9.2 Hz, 1H), 7.23 (s, 1H), 7.15 (dd, J_1 = 6.4 Hz, J_2 = 2.8 Hz, 1H), 7.04 (ddd, J_1 = 8.8 Hz, J_2 = 4.0 Hz, J_3 = 2.8 Hz, 1H), 6.79 (d, J = 8.4 Hz, 1H), 2.13 (s, 3H); HRMS (ESI): m/z, Calcd for $C_{17}H_{14}O_3N_3ClF$ $[M+H]^+$: 362.0702, Found 362.0694.

4.2.9. 4-((3-Chloro-4-fluorophenyl)amino)-6-fluoro-1*H*-indole-2-carboxylic acid

(9i): white solid, yield: 93.0%, mp: 226-229□, ^{1}H-NMR (400 MHz, DMSO-d_6) δ (ppm): 12.83 (s, 1H), 11.78 (s, 1H), 8.59 (s, 1H), 7.37-7.33 (m, 3H), 7.25-7.23 (m, 1H), 6.63 (d, J = 9.2 Hz, 1H), 6.53 (d, J = 12.4 Hz, 1H); HRMS (ESI): *m/z*, Calcd. for $C_{15}H_{10}O_2N_2ClF_2$ $[M+H]^+$: 323.0393, Found 323.0403.

4.2.10. 6-Chloro-4-((3-chloro-4-fluorophenyl)amino)-1*H*-indole-2-carboxylic acid (9j): white solid, yield: 94.0%, mp: 205-207 □, ^{1}H-NMR (400 MHz, DMSO-d_6) δ (ppm): 11.86 (d, J = 1.6 Hz, 1H), 8.63 (brs, 1H), 7.39-7.33 (m, 3H), 7.23 (ddd, J_1 = 8.8 Hz, J_2 = 4.4 Hz, J_3 = 2.8 Hz, 1H), 6.95-6.94 (m, 1H), 6.66 (d, J = 1.6 Hz, 1H); HRMS (ESI): *m/z*, Calcd. for $C_{15}H_{10}O_2N_2Cl_2F$ $[M+H]^+$: 339.0098, Found 339.0103.

4.2.11. 4-((3-Chloro-4-fluorophenyl)amino)-6-methyl-1H-indole-2-carboxylic acid (9k): brown solid, yield: 94.0%, mp: 155-157 □, ^{1}H-NMR (400 MHz, DMSO-d_6) δ (ppm): 11.57 (s, 1H), 8.28 (brs, 1H), 7.29 (t, J = 12.0 Hz, 1H), 7.24 (dd, J_1 = 8.4 Hz, J_2 = 2.8 Hz, 1H), 7.19 (s, 1H), 7.16-7.12 (m, 1H), 6.79 (s, 1H), 6.63 (s, 1H), 2.33 (s, 3H); HRMS (ESI): *m/z*, Calcd. for $C_{16}H_{13}O_2N_2ClF$ $[M+H]^+$: 319.0644, Found 319.0655.

4.2.12. 4-((3-Chloro-4-fluorophenyl)amino)-6-methoxy-1*H*-indole-2-carboxylic acid (9l): celadon solid, yield: 82.6%, mp: 108-110 □, ^{1}H-NMR (400 MHz, DMSO-d_6) δ (ppm): 12.63 (s, 1H), 11.56 (s, 1H), 8.37 (s, 1H), 7.32 (t, J = 9.2 Hz, 1H), 7.29 (dd, J_1 = 6.4 Hz, J_2 = 2.8 Hz, 1H), 7.24-7.23 (m, 1H), 7.18 (ddd, J_1 = 8.8 Hz, J_2 = 4.0 Hz, J_3 = 2.8 Hz, 1H), 6.43 (d, J = 1.2 Hz, 1H), 6.38 (d, J = 2.0 Hz, 1H), 3.74 (s, 3H); HRMS (ESI): *m/z*, Calcd. for $C_{16}H_{13}O_3N_2ClF$ $[M+H]^+$: 335.0593, Found 335.0590.

4.2.13. 4-((3-Chloro-4-fluorophenyl)amino)-6-cyano-1*H*-indole-2-carboxylic acid (9m): khaki solid, yield: 97.8%, mp: >250 □, ^{1}H-NMR (400 MHz, DMSO-d_6) δ (ppm): 13.27 (brs, 1H), 12.27 (s, 1H), 8.66 (s, 1H), 7.43-7.35 (m, 4H), 7.29-7.25 (m, 1H), 6.89 (s, 1H); HRMS (ESI): *m/z*, Calcd. for $C_{16}H_{10}O_2N_3ClF$ $[M+H]^+$: 330.0440, Found 330.0437.

4.2.14. 4-((3-Chloro-4-fluorophenyl)amino)-6-nitro-1*H*-indole-2-carboxylic acid (9n): red-brown solid, yield: 99.4%, mp: >250 □, ^{1}H-NMR (400 MHz, DMSO-d_6) δ (ppm): 11.77 (brs, 1H), 8.60 (s, 1H), 7.90 (d, J = 1.2 Hz, 1H), 7.47 (d, J = 2.0 Hz, 1H), 7.37 (t, J = 8.8 Hz, 1H), 7.35 (dd, J_1 = 6.0 Hz, J_2 = 2.8 Hz, 1H), 7.23 (ddd, J_1 = 8.8 Hz, J_2 = 4.0 Hz, J_3 = 2.8 Hz,1H), 6.90 (s, 1H); ^{13}C-NMR (100 MHz, DMSO-d_6) δ (ppm): 172.87, 164.61, 152.34 (d, J = 238.1 Hz), 143.34, 140.67 (d, J = 2.3 Hz), 136.69, 135.03, 124.76, 120.41, 120.10 (d, J = 18.4 Hz), 119.10 (d, J = 6.6 Hz), 117.75 (d, J = 21.5 Hz), 102.72, 101.84, 97.36; HRMS (ESI): *m/z*, Calcd. for $C_{15}H_{10}O_4N_3ClF$ $[M+H]^+$: 350.0338, Found 350.0336.

4.2.15. 6-Acetamido-4-((3-chloro-4-fluorophenyl)amino)-1*H*-indole-2-carboxylic acid (9o): light brown solid, yield: 96.8%, mp: >250 □, ^{1}H-NMR (400 MHz, DMSO-d_6) δ (ppm): 11.56 (s, 1H), 9.83 (s, 1H), 8.33 (brs, 1H), 7.57 (s, 1H), 7.32 (t, J = 8.8 Hz, 1H), 7.30 (dd, J_1 = 6.4 Hz, J_2 = 2.8 Hz, 1H), 7.23 (d, J = 1.2 Hz, 1H), 7.16 (ddd, J_1 = 8.8 Hz, J_2 = 4.0 Hz, J_3 = 2.8 Hz, 1H), 6.95 (d, J = 1.2 Hz, 1H), 2.02 (s, 3H); HRMS (ESI): *m/z*, Calcd. for $C_{17}H_{14}O_3N_3ClF$ $[M+H]^+$: 362.0702, Found 362.0718.

4.2.16.

4-((3-Chloro-4-fluorophenyl)amino)-6-(ethylamino)-1*H*-indole-2-carboxylic acid (9p): dark green solid, yield: 23.8%, mp: >250 □, ^{1}H-NMR (400 MHz, DMSO-d_6) δ (ppm): 11.00 (s, 1H), 8.12 (s, 1H), 7.27 (t, J = 9.2 Hz, 1H), 7.23 (dd, J_1 = 6.4 Hz, J_2 = 2.4 Hz, 1H), 7.12-7.09 (m, 1H), 7.06 (s, 1H), 6.30 (s, 1H), 6.01 (s, 1H), 2.99 (q, J = 7.2 Hz, 2H), 1.78 (t, J = 7.2 Hz, 3H); HRMS (ESI): *m/z*, Calcd. for $C_{17}H_{16}O_2N_3ClF$ $[M+H]^+$: 348.0910, Found 348.0908.

4.2.17.

4-((3-Chloro-4-fluorophenyl)amino)-7-fluoro-1-methyl-1*H*-indole-2-carboxylic acid (9q): kelly solid, yield: 93.8%, mp: 215-217 □, ^{1}H-NMR (500 MHz, DMSO-d_6) δ (ppm): 13.07 (s, 1H), 8.30 (s, 1H), 7.40 (d, J = 2.5 Hz, 1H), 7.27 (t, J = 11.5 Hz, 1H), 7.17 (dd, J_1 = 8.0 Hz, J_2 = 3.5 Hz, 1H), 7.07-6.99 (m, 2H), 6.74 (dd, J_1 = 10.5 Hz, J_2 = 4.0 Hz, 1H), 4.19 (d, J = 1.5 Hz, 1H); HRMS (ESI): *m/z*, Calcd. for $C_{16}H_{12}O_2N_2ClF_2$

$[M+H]^+$: 337.0550, Found 337.0540.

4.2.18. 4-((3-Chloro-4-fluorophenyl)amino)-1,6-dimethyl-1*H*-indole-2-carboxylic acid (9r): yellow solid, yield: 89.0%, mp: 200-202 □, ^{1}H-NMR (500 MHz, DMSO-d_6) δ (ppm): 12.69 (s, 1H), 8.34 (s, 1H), 7.35 (s, 1H), 7.29 (t, J = 8.0 Hz, 1H), 7.25 (dd, J_1 = 6.5 Hz, J_2 = 2.5 Hz, 1H), 7.16-7.14 (m, 1H), 6.88 (s, 1H), 6.69 (s, 1H), 3.96 (s, 3H), 2.38 (s, 3H); ^{13}C-NMR (100 MHz, DMSO-d_6) δ (ppm): 163.39, 151.76 (d, J = 237.4 Hz), 141.56, 141.34 (d, J = 2.2 Hz), 136.99, 136.02, 126.69, 119.93 (d, J = 18.4 Hz), 119.24, 118.07 (d, J = 6.5 Hz), 117.60 (d, J = 21.4 Hz), 116.14, 108.63, 107.20, 103.70, 31.99, 22.63; HRMS (ESI): *m/z*, Calcd. for $C_{17}H_{15}O_2N_2ClF$ $[M+H]^+$: 333.0801, Found 333.0794.

4.2.19. 6-Acetamido-4-((3-chloro-4-fluorophenyl)amino)benzo[*b*]thiophene-2-carboxylic acid (9s): brown solid, yield: 96.7%, mp: >250 □, ^{1}H-NMR (400 MHz, DMSO-d_6) δ (ppm): 13.21 (brs, 1H), 10.10 (s, 1H), 8.65 (s, 1H), 8.32 (d, J = 0.4 Hz, 1H), 7.95 (s, 1H), 7.38 (t, J = 9.2 Hz, 1H), 7.36 (dd, J_1 = 7.2 Hz, J_2 = 2.8 Hz, 1H), 7.25 (d, J = 1.6 Hz, 1H), 7.21 (ddd, J_1 = 8.8 Hz, J_2 = 4.0 Hz, J_3 = 2.8 Hz,1H), 2.05 (s, 3H); ^{13}C-NMR (100 MHz, DMSO-d_6) δ (ppm): 169.17, 164.02, 152.61 (d, J = 238.8 Hz), 144.59, 140.69, 140.37, 140.25 (d, J = 2.5 Hz), 130.68, 128.26, 125.84, 120.91, 120.18 (d, J = 18.4 Hz), 119.80 (d, J = 6.7 Hz), 117.80 (d, J = 21.6 Hz), 103.91, 101.66, 24.68; HRMS (ESI): *m/z*, Calcd. for $C_{17}H_{13}O_3N_2ClFS$ $[M+H]^+$: 379.0314, Found 379.0306.

4.2.20. 4-((3,4-Difluorophenyl)amino)-7-fluoro-1*H*-indole-2-carboxylic acid (9a-1): khaki solid, yield: 89.1%, mp: >200 □, ^{1}H-NMR (400 MHz, DMSO-d_6) δ (ppm): 13.04 (s, 1H), 12.25 (s, 1H), 8.29 (s, 1H), 7.32-7.23 (m, 2H), 7.02-6.94 (m, 2H), 6.88-6.86 (m, 1H), 6.78-6.73 (m, 1H); HRMS (ESI): *m/z*, Calcd. for $C_{15}H_{10}O_2N_2F_3$ $[M+H]^+$: 307.0689, Found 307.0681.

4.2.21. 4-((3-Bromo-4-fluorophenyl)amino)-7-fluoro-1*H*-indole-2-carboxylic acid (9a-2): yellow solid, yield: 99.7%, mp: 103-105 □, ^{1}H-NMR (400 MHz, DMSO-d_6) δ

(ppm): 13.09 (brs, 1H), 12.27 (s, 1H), 8.32 (s, 1H), 7.32-7.28 (m, 2H), 7.24 (t, J = 8.4 Hz, 1H), 7.09 (ddd, J_1 = 8.8 Hz, J_2 = 4.0 Hz, J_3 = 2.8 Hz, 1H), 6.97 (dd, J_1 = 10.8 Hz, J_2 = 8.4 Hz, 1H), 6.72 (dd, J_1 = 8.4 Hz, J_2 = 3.2 Hz, 1H); ^{13}C-NMR (100 MHz, DMSO-d_6) δ (ppm): 162.78, 152.49 (d, J = 234.9 Hz), 144.99 (d, J = 238.3 Hz), 142.38 (d, J = 2.0 Hz), 133.05 (d, J = 2.6 Hz), 129.04, 127.06 (d, J = 15.3 Hz), 123.37 (d, J = 5.1 Hz), 120.76, 117.65 (d, J = 6.5 Hz), 117.39 (d, J = 22.9 Hz), 109.79 (d, J = 17.3 Hz), 108.44 (d, J = 21.7 Hz), 107.44, 106.03 (d, J = 5.6 Hz); HRMS (ESI): *m/z*, Calcd. for $C_{15}H_{10}O_2N_2BrF_2$ $[M+H]^+$: 366.9888, Found 366.9884.

4.2.22. 7-Fluoro-4-((4-fluoro-3-methoxyphenyl)amino)-1*H*-indole-2-carboxylic acid (9a-3): brown solid, yield: 73.9%, mp: 102-104 □, ^{1}H-NMR (400 MHz, DMSO-d_6) δ (ppm): 12.97 (brs, 1H), 12.16 (s, 1H), 8.10 (s, 1H), 7.35 (t, J = 2.4 Hz, 1H), 7.06 (dd, J_1 = 11.2 Hz, J_2 = 8.8 Hz, 1H), 6.94-6.88 (m, 2H), 6.70 (dd, J_1 = 8.4 Hz, J_2 = 3.2 Hz, 1H), 6.67-6.63 (m, 1H), 3.78 (s, 3H); ^{13}C-NMR (100 MHz, DMSO-d_6) δ (ppm): 162.88, 147.84 (d, J = 11.4 Hz), 146.37 (d, J = 234.5 Hz), 144.39 (d, J = 237.2 Hz), 141.12 (d, J = 2.1 Hz), 134.22 (d, J = 2.5 Hz), 128.72, 127.11 (d, J = 15.2 Hz), 122.77 (d, J = 4.8 Hz), 116.34 (d, J = 18.5 Hz), 109.85 (d, J = 16.7 Hz), 109.22 (d, J = 5.9 Hz), 107.73, 104.37, 104.23 (d, J = 5.2 Hz), 56.21; HRMS (ESI): *m/z*, Calcd. for $C_{16}H_{13}O_3N_2F_2$ $[M+H]^+$: 319.0889, Found 319.0880.

4.2.23. 7-Fluoro-4-((4-fluoro-3-(trifluoromethoxy)phenyl)amino)-1*H*-indole-2-carboxylic acid (9a-4): brown solid, yield: 99.0%, mp: 92-93 □, ^{1}H-NMR (400 MHz, DMSO-d_6) δ 12.27 (s, 1H), 8.39 (s, 1H), 7.34 (t, J = 9.2 Hz, 1H), 7.25 (dd, J_1 = 2.8 Hz, J_2 = 2.4 Hz, 1H), 7.11-7.07 (m, 2H), 6.98 (dd, J_1 = 11.2 Hz, J_2 = 8.4 Hz, 1H), 6.75 (dd, J_1 = 8.4 Hz, J_2 = 3.6 Hz, 1H); HRMS (ESI): *m/z*, Calcd. for $C_{16}H_{10}O_3N_2F_5$ $[M+H]^+$: 373.0606, Found 373.0597.

4.2.24. 4-((3-Cyano-4-fluorophenyl)amino)-7-fluoro-1*H*-indole-2-carboxylic acid (9a-5): light brown solid, yield: 97.9%, mp: >250 □, ^{1}H-NMR (400 MHz, DMSO-d_6) δ (ppm): 13.06 (brs, 1H), 12.27 (s, 1H), 8.45 (s, 1H), 7.39-7.37 (m, 3H), 7.24 (t, J =

2.0 Hz, 1H), 6.98 (dd, J_1 = 11.2 Hz, J_2 = 8.4 Hz, 1H), 6.78 (dd, J_1 = 8.0 Hz, J_2 = 3.2 Hz, 1H); HRMS (ESI): *m/z*, Calcd. for $C_{16}H_{10}O_2N_3F_2$ $[M+H]^+$: 314.0736, Found 314.0726.

4.2.25. 4-((3,4-Dichlorophenyl)amino)-7-fluoro-1*H*-indole-2-carboxylic acid (9a-6): brown solid, yield: 92.0%, mp: 144-145 □, ^{1}H-NMR (400 MHz, DMSO-d_6) δ (ppm): 12.24 (s, 1H), 8.48 (s, 1H), 7.40 (d, *J* = 8.8 Hz, 1H), 7.19-7.18 (m, 2H), 7.02-6.97 (m, 2H), 6.81-6.79 (m, 1H); HRMS (ESI): *m/z*, Calcd. for $C_{15}H_{10}O_2N_2Cl_2F$ $[M+H]^+$: 339.0098, Found 339.0095.

4.2.26. 4-((3-Chloro-4-methoxyphenyl)amino)-7-fluoro-1*H*-indole-2-carboxylic acid (9a-7): brown solid, yield: 32.5%, mp: 131-133 □, ^{1}H-NMR (400 MHz, DMSO-d_6) δ (ppm): 11.95 (s, 1H), 7.97 (s, 1H), 7.23 (brs, 1H), 7.14 (s, 1H), 7.06 (s, 2H), 6.88 (t, *J* = 8.8 Hz, 1H), 6.57 (dd, J_1 = 8.4 Hz, J_2 = 2.0 Hz, 1H), 3.80 (s, 3H); HRMS (ESI): *m/z*, Calcd. for $C_{16}H_{13}O_3N_2ClF$ $[M+H]^+$: 335.0593, Found 335.0584.

4.2.27. 4-((3-Chloro-4-(trifluoromethoxy)phenyl)amino)-7-fluoro-1*H*-indole-2-carboxylic acid (9a-8): black solid, yield: 94.4%, mp: 196-198 □, ^{1}H-NMR (400 MHz, DMSO-d_6) δ (ppm): 13.08 (brs, 1H), 12.32 (s, 1H), 8.55 (s, 1H), 7.36 (d, *J* = 8.8 Hz, 1H), 7.24 (s, 1H), 7.17 (d, *J* = 1.6 Hz, 1H), 7.06-6.99 (m, 2H), 6.84 (dd, J_1 = 8.0 Hz, J_2 = 2.4 Hz, 1H); HRMS (ESI): *m/z*, Calcd. for $C_{16}H_{10}O_3N_2ClF_4$ $[M+H]^+$: 389.0311, Found 389.0303.

4.2.28. 4-((3-Chloro-4-(trifluoromethyl)phenyl)amino)-7-fluoro-1*H*-indole-2-carboxylic acid (9a-9): brown solid, yield: 92.5%, mp: 83-85 □, ^{1}H-NMR (400 MHz, DMSO-d_6) δ (ppm): 13.13 (brs, 1H), 12.40 (s, 1H), 8.90 (s, 1H), 7.59 (d, *J* = 8.8 Hz, 1H), 7.16 (t, *J* = 2.4 Hz, 1H), 7.12 (d, *J* = 2.4 Hz, 1H), 7.06 (dd, J_1 = 10.8 Hz, J_2 = 8.0 Hz, 1H), 6.99 (dd, J_1 = 8.4 Hz, J_2 = 2.0 Hz, 1H), 6.92 (dd, J_1 = 8.4 Hz, J_2 = 3.6 Hz, 1H); HRMS (ESI): *m/z*, Calcd. for $C_{16}H_{10}O_2N_2ClF_4$ $[M+H]^+$: 373.0361, Found 373.0348.

4.2.29.

7-Fluoro-4-((3-methoxy-5-(trifluoromethyl)phenyl)amino)-1*H*-indole-2-carboxylic acid (9a-10): yellowish white solid, yield: 86%, mp: 99-101 □, ^{1}H-NMR (400 MHz, DMSO-d_6) δ (ppm): 12.25 (s, 1H), 8.51 (s, 1H), 7.22 (s, 1H), 7.03-6.98 (m, 1H), 6.91 (s, 1H), 6.84 (d, J = 3.2 Hz, 1H), 6.82 (s, 1H), 6.61 (s, 1H), 3.76 (s, 3H); HRMS (ESI): *m/z*, Calcd. for $C_{17}H_{13}O_3N_2F_4$ $[M+H]^+$: 369.0857, Found 369.0839.

4.2.30. 4-((3-Chloro-5-methoxyphenyl)amino)-7-fluoro-1*H*-indole-2-carboxylic acid (9a-11): yellow solid, yield: 81.3%, mp: 108-110 □, ^{1}H-NMR (400 MHz, DMSO-d_6) δ (ppm): 13.07 (brs, 1H), 12.25 (s, 1H), 8.35 (s, 1H), 7.24 (t, J = 2.0 Hz, 1H), 6.99 (dd, J_1 = 10.4 Hz, J_2 = 8.4 Hz, 1H), 6.81 (dd, J_1 = 8.4 Hz, J_2 = 3.2 Hz, 1H), 6.64 (t, J = 1.2 Hz, 1H), 6.54 (t, J = 1.6 Hz, 1H), 6.42 (t, J = 1.6 Hz, 1H), 3.71 (s, 3H); ^{13}C-NMR (100 MHz, DMSO-d_6) δ (ppm): 162.81, 161.35, 147.27, 145.38 (d, J = 239.2 Hz), 134.59, 132.14 (d, J = 2.8 Hz), 129.30, 127.00 (d, J = 15.3 Hz), 124.12 (d, J = 5.1 Hz), 109.73 (d, J = 17.3 Hz), 108.43, 108.21 (d, J = 5.8 Hz), 107.39, 105.00, 100.47, 55.76; HRMS (ESI): *m/z*, Calcd. for $C_{16}H_{13}O_3N_2ClF$ $[M+H]^+$: 335.0593, Found 335.0578.

4.2.31. 4-((5-Bromo-2-fluorophenyl)amino)-7-fluoro-1*H*-indole-2-carboxylic acid (9a-12): light-brown solid, yield: 99.5%, mp: 204-205 □, ^{1}H-NMR (400 MHz, DMSO-d_6) δ (ppm): 13.10 (brs, 1H), 12.32 (s, 1H), 8.17 (s, 1H), 7.20 (dd, J_1 = 11.6 Hz, J_2 = 8.4 Hz, 1H), 7.14 (dd, J_1 = 2.8 Hz, J_2 = 2.4 Hz, 1H), 7.06-6.98 (m, 3H), 6.59 (dd, J_1 = 8.4 Hz, J_2 = 3.2 Hz, 1H); ^{13}C-NMR (100 MHz, DMSO-d_6) δ (ppm): 162.76, 152.57 (d, J = 241.8 Hz), 145.82 (d, J = 239.7 Hz), 134.87 (d, J = 12.6 Hz), 132.09 (d, J = 2.9 Hz), 129.35, 126.94 (d, J = 15.3 Hz), 124.13 (d, J = 5.3 Hz), 123.00 (d, J = 7.1 Hz), 121.13 (d, J = 3.3 Hz), 118.12 (d, J = 20.4 Hz), 116.60 (d, J = 2.8 Hz), 109.77 (d, J = 17.3 Hz), 109.33 (d, J = 5.7 Hz), 107.41; HRMS (ESI): *m/z*, Calcd. for $C_{15}H_{10}O_2N_2BrF_2$ $[M+H]^+$: 366.9888, Found 366.9883.

4.2.32. 4-((2-Carboxy-5-methoxyphenyl)amino)-7-fluoro-1H-indole-2-carboxylic acid (9a-13): brown solid, yield: 98.8%, mp: 215-217 □, ^{1}H-NMR (400 MHz, DMSO-d_6) δ 12.00 (s, 1H), 7.90 (d, J = 8.8 Hz, 1H), 7.00-6.94 (m, 2H), 6.92 (d, J =

2.8 Hz, 1H), 6.66 (d, J = 2.4 Hz, 1H), 6.33 (dd, J_1 = 8.8 Hz, J_2 = 2.4 Hz, 1H), 3.69 (s, 3H); ^{13}C-NMR (100 MHz, DMSO-d_6) δ (ppm): 171.23, 163.68, 163.54, 149.24, 145.97 (d, J = 239.9 Hz), 134.21, 133.42, 130.71 (d, J = 2.4 Hz), 126.12 (d, J = 15.1 Hz), 125.49 (d, J = 5.5 Hz), 109.74 (d, J = 4.5 Hz), 108.81 (d, J = 17.0 Hz), 104.56, 104.01, 98.10, 55.48; HRMS (ESI): *m/z*, Calcd. for $C_{17}H_{14}O_5N_2F$ $[M+H]^+$: 345.0881, Found 345.0878.

4.2.33. 7-Fluoro-4-((3,4,5-trimethoxyphenyl)amino)-1*H*-indole-2-carboxylic acid (9a-14): brown solid, yield: 64.7%, mp: 251-253 □, ^{1}H-NMR (500 MHz, DMSO-d_6) δ (ppm): 12.13 (brs, 1H), 8.03 (s, 1H), 7.38 (s, 1H), 6.92 (t, J = 9.0 Hz, 1H), 6.74 (dd, J_1 = 8.5 Hz, J_2 = 4.5 Hz, 1H), 6.45 (s, 2H), 3.71 (s, 6H), 3.61 (s, 3H); HRMS (ESI): *m/z*, Calcd. for $C_{18}H_{18}O_5N_2F$ $[M+H]^+$: 361.1194, Found 361.1184.

4.2.34. 4-((1*H*-indol-4-yl)amino)-7-fluoro-1*H*-indole-2-carboxylic acid (9a-15): brown solid, yield: 91.7%, mp: >250 □, ^{1}H-NMR (400 MHz, DMSO-d_6) δ (ppm): 12.90 (brs, 1H), 12.07 (s, 1H), 11.00 (s, 1H), 7.92 (s, 1H), 7.37 (t, J = 2.4 Hz, 1H), 7.21 (t, J = 2.8 Hz, 1H), 6.98 (t, J = 8.0 Hz, 1H), 6.94 (t, J = 8.0 Hz, 1H), 6.89 (dd, J_1 = 10.8 Hz, J_2 = 8.4 Hz, 1H), 6.67 (d, J = 6.8 Hz, 1H), 6.54 (dd, J_1 = 8.0 Hz, J_2 = 3.2 Hz, 1H), 6.50 (t, J = 2.0 Hz, 1H); HRMS (ESI): m/z, Calcd for $C_{17}H_{13}O_2N_3F$ $[M+H]^+$: 310.0986, Found 310.0984.

4.2.35. 7-Fluoro-4-((7-fluoro-1*H*-indol-4-yl)amino)-1*H*-indole-2-carboxylic acid (9a-16): brown solid, yield: 95.6%, mp: >250 □, ^{1}H-NMR (400 MHz, DMSO-d_6) δ (ppm): 12.07 (d, J = 1.6 Hz, 1H), 11.52 (s, 1H), 7.39 (dd, J_1 = 2.8 Hz, J_2 = 2.4 Hz, 1H), 7.29 (t, J = 2.8 Hz, 1H), 6.93-6.77 (m, 3H), 6.62 (dd, J_1 = 8.4 Hz, J_2 = 3.6 Hz, 1H), 6.50 (td, J_1 = 3.2 Hz, J_2 = 2.0 Hz, 1H), 6.38 (dd, J_1 = 8.4 Hz, J_2 = 3.2 Hz, 1H); HRMS (ESI): m/z, Calcd for $C_{17}H_{12}O_2N_3F_2$ $[M+H]^+$: 328.0892, Found 328.0888.

4.2.36. 4,4'-Azanediylbis(7-fluoro-1*H*-indole-2-carboxylic acid) (9a-17): black solid, yield: 92.2%, mp: >250 □, ^{1}H-NMR (400 MHz, DMSO-d_6) δ (ppm): 13.00 (brs, 2H), 12.15 (s, 2H), 8.09 (brs, 1H), 7.35 (s, 2H), 6.92 (dd, J_1 = 10.8 Hz, J_2 = 8.4 Hz, 2H), 6.59 (dd, J_1 = 8.4 Hz, J_2 = 3.2 Hz, 2H); ^{13}C-NMR (100 MHz, DMSO-d_6) δ (ppm): 162.88, 144.61 (d, J = 237.2 Hz), 134.53 (d, J = 2.5 Hz), 128.68, 127.07 (d, J

= 15.1 Hz), 123.21 (d, *J* = 4.8 Hz), 109.75 (d, *J* = 17.1 Hz), 108.10, 106.30 (d, *J* = 5.5 Hz); HRMS (ESI): *m/z*, Calcd. for $C_{18}H_{12}O_4N_3F_2$ $[M+H]^+$: 372.0790, Found 370.0790.

4.2.37. 6-Acetamido-4-((3,4-difluorophenyl)amino)-1*H*-indole-2-carboxylic acid (9o-1): brown solid, yield: 84.3%, mp: >250 □, ^{1}H-NMR (400 MHz, DMSO-d_6) δ (ppm): 12.69 (brs, 1H), 11.55 (d, *J* = 1.6 Hz, 1H), 9.82 (s, 1H), 8.35 (s, 1H), 7.57 (s, 1H), 7.33 (dd, J_1 = 20.0 Hz, J_2 = 9.2 Hz, 1H), 7.25 (d, *J* = 1.6 Hz, 1H), 7.17 (ddd, J_1 = 13.2 Hz, J_2 = 7.2 Hz, J_3 = 2.4 Hz, 1H), 7.01-6.96 (m, 2H), 2.02 (s, 3H); HRMS (ESI): *m/z*, Calcd. for $C_{17}H_{14}O_3N_3F_2$ $[M+H]^+$: 346.0998, Found 346.0990.

4.2.38.

6-Acetamido-4-((4-fluoro-3-methoxyphenyl)amino)-1*H*-indole-2-carboxylic acid (9o-2): gray solid, yield: 95.1%, mp: 240-242 □, ^{1}H-NMR (400 MHz, DMSO-d_6) δ (ppm): 11.48 (s, 1H), 9.78 (s, 1H), 8.17 (brs, 1H), 7.44 (s, 1H), 7.31-7.30 (m, 1H), 7.11 (ddd, J_1 = 11.2 Hz, J_2 = 8.8 Hz, J_3 = 0.8 Hz, 1H), 7.03 (dd, J_1 = 8.0 Hz, J_2 = 2.0 Hz, 1H), 7.00 (s, 1H), 6.76-6.72 (m, 1H), 3.83 (s, 3H), 2.01 (s, 3H); ^{13}C-NMR (100 MHz, DMSO-d_6) δ (ppm): 168.48, 163.14, 147.68 (d, *J* = 11.2 Hz), 146.67 (d, *J* = 235.1 Hz), 140.10 (d, *J* = 2.1 Hz), 139.30, 138.00, 137.97, 126.37, 116.32 (d, *J* = 18.5 Hz), 115.43, 110.70 (d, *J* = 6.1 Hz), 106.87, 105.43, 96.78, 94.37, 56.16, 24.63; HRMS (ESI): *m/z*, Calcd. for $C_{18}H_{17}O_4N_3F$ $[M+H]^+$: 358.1198, Found 358.1194.

4.2.39. 6-Acetamido-4-((3-ethoxy-4-fluorophenyl)amino)-1*H*-indole-2-carboxylic acid (9o-3): light brown solid, yield: 71.0%, mp: 220-222 □, ^{1}H-NMR (400 MHz, DMSO-d_6) δ (ppm): 11.44 (s, 1H), 9.78 (s, 1H), 8.12 (s, 1H), 7.46 (s, 1H), 7.26 (d, *J* = 1.2 Hz, 1H), 7.10 (dd, J_1 = 11.2 Hz, J_2 = 8.8 Hz, 1H), 6.99 (dd, J_1 = 8.0 Hz, J_2 = 2.4 Hz, 1H), 6.95 (d, *J* = 1.2 Hz, 1H), 6.74 (ddd, J_1 = 8.8 Hz, J_2 = 3.6 Hz, J_3 = 2.8 Hz, 1H), 4.08 (q, *J* = 7.2 Hz, 2H), 2.01 (s, 3H), 1.35 (t, *J* = 7.2 Hz, 3H); HRMS (ESI): *m/z*, Calcd. for $C_{19}H_{19}O_4N_3F$ $[M+H]^+$: 372.1354, Found 372.1349.

4.2.40.

6-Acetamido-4-((4-fluoro-3-propoxyphenyl)amino)-1*H*-indole-2-carboxylic acid (9o-4): brown solid, yield: 99.0%, mp: 248-250 □, ^{1}H-NMR (400 MHz, DMSO-d_6) δ

(ppm): 11.48 (s, 1H), 9.77 (s, 1H), 8.13 (s, 1H), 7.45 (s, 1H), 7.29 (d, J = 1.2 Hz, 1H), 7.11 (dd, J_1 = 11.2 Hz, J_2 = 8.8 Hz, 1H), 6.99 (dd, J_1 = 7.6 Hz, J_2 = 2.4 Hz, 1H), 6.96 (d, J = 1.2 Hz, 1H), 6.74 (ddd, J_1 = 8.8 Hz, J_2 = 3.6 Hz, J_3 = 2.4 Hz, 1H), 3.98 (t, J = 7.2 Hz, 2H), 2.01 (s, 3H), 1.80-1.71 (m, 2H), 0.985 (t, J = 7.2 Hz, 3H); ^{13}C-NMR (100 MHz, DMSO-d_6) δ (ppm): 168.43, 163.11, 147.09 (d, J = 11.4 Hz), 146.90 (d, J = 235.4 Hz), 140.02 (d, J = 1.9 Hz), 139.28, 138.03, 137.95, 126.34, 116.34 (d, J = 18.6 Hz), 115.40, 110.75 (d, J = 6.2 Hz), 106.84, 106.57, 96.79, 94.38, 70.32, 24.61, 22.46, 10.75; HRMS (ESI): *m/z*, Calcd. for $C_{20}H_{21}O_4N_3F$ $[M+H]^+$: 386.1511, Found 386.1503.

4.2.41.

6-Acetamido-4-((4-fluoro-3-(trifluoromethoxy)phenyl)amino)-1*H*-indole-2-carbo xylic acid (9o-5): gray solid, yield: 93.4%, mp: 239-241 □, ^{1}H-NMR (400 MHz, DMSO-d_6) δ (ppm): 12.67 (brs, 1H), 11.58 (s, 1H), 9.83 (s, 1H), 8.44 (s, 1H), 7.55 (s, 1H), 7.40 (t, J = 9.6 Hz, 1H), 7.25-7.21 (m, 3H), 7.01 (s, 1H), 2.02 (s, 3H); HRMS (ESI): *m/z*, Calcd. for $C_{18}H_{14}O_4N_3F_4$ $[M+H]^+$: 412.0915, Found 412.0908.

4.2.42.

6-Acetamido-4-((4-fluoro-3-isopropoxyphenyl)amino)-1*H*-indole-2-carboxylic acid (9o-6): light brown solid, yield: 99.6%, mp: 163-165 □, ^{1}H-NMR (400 MHz, DMSO-d_6) δ (ppm): 12.56 (brs, 1H), 11.47 (s, 1H), 9.77 (s, 1H), 8.10 (s, 1H), 7.46 (s, 1H), 7.26 (d, J = 1.2 Hz, 1H), 7.11 (dd, J_1 = 11.2 Hz, J_2 = 8.8 Hz, 1H), 6.95 (dd, J_1 = 8.0 Hz, J_2 = 2.8 Hz, 1H), 6.91 (d, J = 0.8 Hz, 1H), 6.77 (ddd, J_1 = 8.8 Hz, J_2 = 3.6 Hz, J_3 = 2.8 Hz, 1H), 4.57-4.51 (m, 1H), 2.00 (s, 3H), 1.29 (d, J = 6.0 Hz, 6H); ^{13}C-NMR (100 MHz, DMSO-d_6) δ (ppm): 168.43, 163.18, 147.83 (d, J = 235.4 Hz), 145.85 (d, J = 11.3 Hz), 140.06 (d, J = 1.7 Hz), 139.25, 138.07, 137.90, 126.57, 116.59 (d, J = 19.3 Hz), 115.46, 111.27 (d, J = 6.4 Hz), 108.65, 106.76, 96.93, 94.51, 71.72, 24.61, 22.38; HRMS (ESI): *m/z*, Calcd. for $C_{20}H_{21}O_4N_3F$ $[M+H]^+$: 386.1511, Found 386.1503.

4.2.43.

6-Acetamido-4-((3-(cyclopropylmethoxy)-4-fluorophenyl)amino)-1*H*-indole-2-car

boxylic acid (9o-7): brown solid, yield: 99.4%, mp: 244-246 □, ^{1}H-NMR (400 MHz, DMSO-d_6) δ (ppm): 12.58 (brs, 1H), 11.48 (s, 1H), 9.77 (s, 1H), 8.12 (s, 1H), 7.44 (s, 1H), 7.29 (s, 1H), 7.11 (dd, J_1 = 11.2 Hz, J_2 = 8.8 Hz, 1H), 6.99-6.96 (m, 2H), 6.76-6.72 (m, 1H), 3.87 (d, J = 6.8 Hz, 2H), 2.00 (s, 3H), 1.27-1.23 (m, 1H), 0.60-0.56 (m, 2H), 0.35-0.31 (m, 2H); HRMS (ESI): *m/z*, Calcd. for $C_{21}H_{21}O_4N_3F$ $[M+H]^+$: 398.1511, Found 398.1507.

4.2.44.

6-Acetamido-4-((4-fluoro-3-(2,2,2-trifluoroethoxy)phenyl)amino)-1*H*-indole-2-carboxylic acid (9o-8): light brown solid, yield: 59.4%, mp: 250-251 □, ^{1}H-NMR (400 MHz, DMSO-d_6) δ (ppm): 11.51 (d, J = 2.0 Hz, 1H), 9.80 (s, 1H), 8.25 (s, 1H), 7.44 (s, 1H), 7.29 (dd, J_1 = 2.0 Hz, J_2 = 0.4 Hz, 1H), 7.20 (dd, J_1 = 11.2 Hz, J_2 = 8.8 Hz, 1H), 7.13 (dd, J_1 = 7.6 Hz, J_2 = 2.8 Hz, 1H), 7.02 (d, J = 1.6 Hz, 1H), 6.85 (ddd, J_1 = 8.8 Hz, J_2 = 3.6 Hz, J_3 = 2.8 Hz, 1H), 4.81 (q, J = 8.8 Hz, 2H), 2.01 (s, 3H); HRMS (ESI): *m/z*, Calcd. for $C_{19}H_{16}O_4N_3F_4$ $[M+H]^+$: 426.1072, Found 426.1061.

4.2.45.

6-Acetamido-4-((4-fluoro-3-phenoxyphenyl)amino)-1*H*-indole-2-carboxylic acid (9o-9): brown solid, yield: 99.6%, mp: 170-172 □, ^{1}H-NMR (400 MHz, DMSO-d_6) δ (ppm): 11.50 (d, J = 1.6 Hz, 1H), 9.83 (s, 1H), 8.26 (s, 1H), 7.50 (s, 1H), 7.40-7.35 (m, 2H), 7.29 (dd, J_1 = 10.4 Hz, J_2 = 9.2 Hz, 1H), 7.21 (d, J = 1.2 Hz, 1H), 7.12 (t, J = 7.2 Hz, 1H), 7.06-7.01 (m, 3H), 6.95 (d, J = 1.2 Hz, 1H), 6.89 (dd, J_1 = 7.2 Hz, J_2 = 2.8 Hz, 1H), 2.03 (s, 3H); HRMS (ESI): *m/z*, Calcd. for $C_{23}H_{19}O_4N_3F$ $[M+H]^+$: 420.1354, Found 420.1344.

4.2.46.

6-Acetamido-4-((3-(benzyloxy)-4-fluorophenyl)amino)-1*H*-indole-2-carboxylic acid (9o-10): brown solid, yield: 99.4%, mp: 157-159 □, ^{1}H-NMR (400 MHz, DMSO-d_6) δ (ppm): 11.49 (d, J = 1.6 Hz, 1H), 9.82 (s, 1H), 7.47-7.30 (m, 7H), 7.16-7.11 (m, 2H), 6.99 (d, J = 1.6 Hz, 1H), 6.77 (ddd, J_1 = 8.8 Hz, J_2 = 3.6 Hz, J_3 = 2.8 Hz, 1H), 5.16 (s, 2H), 2.02 (s, 3H); ^{13}C-NMR (100 MHz, DMSO-d_6) δ (ppm): 168.63, 163.16, 146.93 (d, J = 235.2 Hz), 146.86 (d, J = 11.5 Hz), 140.19 (d, J = 1.8

Hz), 139.34, 138.03, 137.93, 137.18, 129.02, 128.55, 128.32, 126.44, 116.54 (d, J = 18.8 Hz), 115.55, 111.20 (d, J = 5.9 Hz), 107.01, 106.78, 97.12, 94.60, 70.66, 24.69; HRMS (ESI): *m/z*, Calcd. for $C_{24}H_{21}O_4N_3F$ $[M+H]^+$: 434.1511, Found 434.1500.

4.2.47. 6-Acetamido-4-((4-fluoro-3-methylphenyl)amino)-1*H*-indole-2-carboxylic acid (9o-11): light brown solid, yield: 99.6%, mp: 230-232 □, ^{1}H-NMR (400 MHz, DMSO-d_6) δ (ppm): 12.64 (brs, 1H), 11.49 (d, J = 1.6 Hz, 1H), 9.77 (s, 1H), 8.08 (brs, 1H), 7.51 (s, 1H), 7.30-7.29 (m, 1H), 7.11 (dd, J_1 = 6.8 Hz, J_2 = 2.4 Hz, 1H), 7.10-7.04 (m, 2H), 6.80 (d, J = 1.6 Hz, 1H), 2.22 (d, J = 1.6 Hz, 3H), 2.01 (s, 3H); ^{13}C-NMR (100 MHz, DMSO-d_6) δ (ppm):168.42, 163.11, 155.96 (d, J = 234.8 Hz), 139.32, 139.30, 138.47, 137.93, 126.26, 124.90 (d, J = 18.0 Hz), 122.69 (d, J = 4.4 Hz), 118.62 (d, J = 7.7 Hz), 115.73, 115.43 (d, J = 15.5 Hz), 106.93, 96.43, 94.27, 24.60, 14.92 (d, J = 3.0 Hz); HRMS (ESI): *m/z*, Calcd. for $C_{18}H_{17}O_3N_3F$ $[M+H]^+$: 342.1249, Found 342.1249.

4.2.48. 6-Acetamido-4-((3-cyclopropyl-4-fluorophenyl)amino)-1*H*-indole-2-carboxylic acid (9o-12): light brown solid, yield: 89.7%, mp: >250 □, ^{1}H-NMR (400 MHz, DMSO-d_6) δ (ppm): 12.60 (s, 1H), 11.48 (s, 1H), 9.79 (s, 1H), 8.06 (s, 1H), 7.42 (s, 1H), 7.28 (s, 1H), 7.07 (t, J = 8.8 Hz, 1H), 7.03-6.97 (m, 1H), 6.87 (s, 1H), 6.77 (dd, J_1 = 6.4 Hz, J_2 = 2.4 Hz, 1H), 2.05-2.00 (m, 4H), 0.99-0.95 (m, 2H), 0.74-0.70 (m, 2H); HRMS (ESI): *m/z*, Calcd. for $C_{20}H_{19}O_3N_3F$ $[M+H]^+$: 368.1405, Found 368.1401.

4.2.49. 6-Acetamido-4-((4-fluoro-3-(thiophen-3-yl)phenyl)amino)-1*H*-indole-2-carboxylic acid (9o-13): light brown solid, yield: 98.3%, mp: 192-194 □, ^{1}H-NMR (400 MHz, DMSO-d_6) δ (ppm): 11.50 (d, J = 2.0 Hz, 1H), 9.83 (s, 1H), 7.87-7.85 (m, 1H), 7.67 (dd, J_1 = 4.8 Hz, J_2 = 3.2 Hz, 1H), 7.52 (dd, J_1 = 7.2 Hz, J_2 = 2.8 Hz, 1H), 7.49 (t, J = 1.6 Hz, 1H), 7.48 (s, 1H), 7.32 (dd, J_1 = 2.0 Hz, J_2 = 0.8 Hz, 1H), 7.24 (dd, J_1 = 10.8 Hz, J_2 = 8.8 Hz, 1H), 7.18 (ddd, J_1 = 8.8 Hz, J_2 = 4.4 Hz, J_3 = 2.8 Hz, 1H), 6.99 (d, J = 1.6 Hz, 1H), 2.01 (s, 3H); HRMS (ESI): *m/z*, Calcd. for $C_{21}H_{17}O_3N_3FS$ $[M+H]^+$: 410.0969, Found 410.0966.

4.2.50. 6-Acetamido-4-((4-fluorophenyl)amino)-1*H*-indole-2-carboxylic acid

(9o-14): brown solid, yield: 95.7%, mp: 224-226 □, ^{1}H-NMR (400 MHz, DMSO-d_6) δ (ppm): 11.48 (d, J = 1.6 Hz, 1H), 9.76 (s, 1H), 8.14 (s, 1H), 7.51 (s, 1H), 7.29 (d, J = 1.6 Hz, 1H), 7.25-7.20 (m, 2H), 7.16-7.11 (m, 2H), 6.83 (d, J = 1.2 Hz, 1H), 2.00 (s, 3H); HRMS (ESI): m/z, Calcd for $C_{17}H_{15}O_3N_3F$ $[M+H]^+$: 328.1092, Found 328.1090.

4.2.51. 6-Acetamido-4-((3,4,5-trimethoxyphenyl)amino)-1*H*-indole-2-carboxylic acid (9o-15): brown solid, yield: 95.7%, mp: 228-229 □, ^{1}H-NMR (400 MHz, DMSO-d_6) δ (ppm): 11.41 (d, J = 1.2 Hz, 1H), 9.70 (s, 1H), 7.45 (s, 1H), 7.32 (d, J = 1.6 Hz, 1H), 7.19-7.15 (m, 2H), 6.94-6.90 (m, 2H), 6.66 (d, J = 1.6 Hz, 1H), 3.74 (s, 3H), 1.98 (s, 3H); ^{13}C-NMR (100 MHz, DMSO-d_6) δ (ppm): 168.43, 163.18, 154.82, 139.66, 139.37, 138.11, 136.09, 126.07, 122.60, 114.93, 114.91, 107.10, 95.13, 93.57, 55.76, 24.60; HRMS (ESI): *m/z*, Calcd. for $C_{18}H_{18}O_4N_3$ $[M+H]^+$: 340.1292, Found 340.1286.

4.2.52.

6-Acetamido-4-((4-(difluoromethoxy)phenyl)amino)-1*H*-indole-2-carboxylic acid (9o-16): brown solid, yield: 99.5%, mp: 199-201 □,^{1}H-NMR (400 MHz, DMSO-d_6) δ (ppm): 11.50 (d, J = 1.6 Hz, 1H), 9.79 (s, 1H), 7.53 (s, 1H), 7.29 (dd, J_1 = 2.0 Hz, J_2 = 0.8 Hz, 1H), 7.26-7.22 (m, 2H), 7.13-7.10 (m, 2H), 7.11 (t, J = 74.8 Hz, 1H), 6.91 (d, J = 1.6 Hz, 1H), 2.01 (s, 3H); HRMS (ESI): *m/z*, Calcd. for $C_{18}H_{16}O_4N_3F_2$ $[M+H]^+$: 376.1103, Found 376.1096.

4.2.53.

6-Acetamido-4-((4-(trifluoromethoxy)phenyl)amino)-1*H*-indole-2-carboxylic acid (9o-17): kelly solid, yield: 92.9%, mp: 244-246 □, ^{1}H-NMR (400 MHz, DMSO-d_6) δ (ppm): 11.54 (s, 1H), 9.82 (s, 1H), 8.38 (s, 1H), 7.58 (s, 1H), 7.26 (s, 5H), 6.98 (d, J = 1.6 Hz, 1H), 2.02 (s, 3H); HRMS (ESI): *m/z*, Calcd. for $C_{18}H_{15}O_4N_3F_3$ $[M+H]^+$: 394.1009, Found 394.1003.

4.2.54.

6-Acetamido-4-((4-(trifluoromethyl)phenyl)amino)-1*H*-indole-2-carboxylic acid (9o-18): light green solid, yield: 82.4%, mp: >250 □, ^{1}H-NMR (400 MHz, DMSO-d_6) δ (ppm): 11.62 (s, 1H), 9.88 (s, 1H), 8.71 (s, 1H), 7.64 (s, 1H), 7.56 (d, J = 8.4 Hz,

2H), 7.27 (d, *J* = 8.4 Hz, 2H), 7.19 (d, *J* = 1.6 Hz, 1H), 7.13 (d, *J* = 0.8 Hz, 1H), 2.02 (s, 3H); HRMS (ESI): *m/z*, Calcd. for $C_{18}H_{15}O_3N_3F_3$ $[M+H]^+$: 378.1060, Found 378.1050.

4.2.55. 6-Acetamido-4-((6-fluoropyridin-3-yl)amino)-1*H*-indole-2-carboxylic acid (9o-19): brown solid, yield: 98.2%, mp: 209-211 □, ^{1}H-NMR (400 MHz, DMSO-d_6) δ (ppm): 11.56 (s, 1H), 9.81 (s, 1H), 8.36 (s, 1H), 8.09 (dd, J_1 = 2.4 Hz, J_2 = 1.6 Hz, 1H), 7.81-7.76 (m, 1H), 7.56 (s, 1H), 7.27 (d, *J* = 1.2 Hz, 1H), 7.13 (dd, J_1 = 8.8 Hz, J_2 = 3.2 Hz, 1H), 6.87 (d, *J* = 1.6 Hz, 1H), 2.01 (s, 3H); ^{13}C-NMR (100 MHz, DMSO-d_6) δ (ppm): 168.51, 163.09, 157.85 (d, *J* = 228.0 Hz), 139.33, 138.42 (d, *J* = 4.0 Hz), 137.86, 137.42 (d, *J* = 6.4 Hz), 137.30, 132.42 (d, *J* = 7.5 Hz), 126.69, 115.50, 109.94 (d, *J* = 39.5 Hz), 106.70, 96.97, 95.18, 24.62; HRMS (ESI): m/z, Calcd for $C_{16}H_{14}O_3N_4F$ $[M+H]^+$: 329.1045, Found 329.1043.

4.2.56. 6-Acetamido-4-((5-fluoropyridin-2-yl)amino)-1*H*-indole-2-carboxylic acid (9o-20): brown solid, yield: 60.5%, mp: 224-226 □, ^{1}H-NMR (400 MHz, DMSO-d_6) δ (ppm): 11.56 (s, 1H), 9.90 (s, 1H), 9.02 (s, 1H), 8.16 (d, *J* = 2.8 Hz, 1H), 7.81 (d, *J* = 1.2 Hz, 1H), 7.73 (s, 1H), 7.63 (td, J_1 = 8.8 Hz, J_2 = 3.2 Hz, 1H), 7.44 (d, *J* = 1.2 Hz, 1H), 7.19 (dd, J_1 = 9.2 Hz, J_2 = 3.6 Hz, 1H), 2.05 (s, 3H); HRMS (ESI): m/z, Calcd for $C_{16}H_{14}O_3N_4F$ $[M+H]^+$: 329.1045, Found 329.1043.

4.2.57. 6-Acetamido-4-((6-methoxypyridin-3-yl)amino)-1*H*-indole-2-carboxylic acid (9o-21): brown solid, yield: 82.6%, mp: 239-240 □, ^{1}H-NMR (400 MHz, DMSO-d_6) δ (ppm): 11.47 (s, 1H), 9.74 (s, 1H), 8.10 (d, *J* = 2.4 Hz, 1H), 7.63 (dd, J_1 = 8.8 Hz, J_2 = 2.8 Hz, 1H), 7.50 (s, 1H), 7.32 (d, *J* = 1.6 Hz, 1H), 6.85 (d, *J* = 8.8 Hz, 1H), 6.62 (d, *J* = 1.2 Hz, 1H), 3.85 (s, 3H), 1.99 (s, 3H); HRMS (ESI): m/z, Calcd for $C_{17}H_{17}O_4N_4$ $[M+H]^+$: 341.1244, Found 341.1244.

4.2.58. 6-Acetamido-4-((5-methoxypyridin-2-yl)amino)-1*H*-indole-2-carboxylic acid (9o-22): brown solid, yield: 94.7%, mp: 239-240 □, ^{1}H-NMR (400 MHz, DMSO-d_6) δ (ppm): 11.79 (s, 1H), 10.12 (s, 1H), 7.83 (s, 1H), 7.77 (s, 2H), 7.47 (s, 1H), 7.29 (d, *J* = 10.0 Hz, 1H), 7.13 (s, 1H), 3.82 (s, 3H), 2.07 (s, 3H); HRMS (ESI):

m/z, Calcd for $C_{17}H_{17}O_4N_4$ $[M+H]^+$: 341.1244, Found 341.1242.

4.2.59. 6-Acetamido-4-((3,4,5-trimethoxyphenyl)amino)-1*H*-indole-2-carboxylic acid (9o-23): brown solid, yield: 83.5%, mp: >250 □, ^{1}H-NMR (400 MHz, DMSO-d_6) δ (ppm): 12.61 (s, 1H), 11.49 (s, 1H), 9.81 (s, 1H), 8.14 (s, 1H), 7.38 (s, 1H), 7.34 (s, 1H), 7.14 (s, 1H), 6.58 (s, 2H), 3.77 (s, 6H), 3.62 (s, 3H), 2.01 (s, 3H); HRMS (ESI): *m/z*, Calcd. for $C_{20}H_{22}O_6N_3$ $[M+H]^+$: 400.1503, Found 400.1498.

4.2.60. 4-((1*H*-indazol-4-yl)amino)-6-acetamido-1*H*-indole-2-carboxylic acid (9o-24): brown solid, yield: 99.0%, mp: >250 □, ^{1}H-NMR (400 MHz, DMSO-d_6) δ (ppm): 11.55 (s, 1H), 9.83 (s, 1H), 8.17 (s, 1H), 7.64 (s, 1H), 7.27 (dd, J_1 = 2.0 Hz, J_2 = 0.4 Hz, 1H), 7.20 (t, J = 8.0 Hz, 1H), 7.02 (d, J = 8.0 Hz, 1H), 6.99 (d, J = 1.2 Hz, 1H), 6.80 (d, J = 7.6 Hz, 1H), 2.01 (s, 3H); ^{13}C-NMR (100 MHz, DMSO-d_6) δ (ppm): 168.54, 163.15, 142.03, 139.39, 137.71, 137.14, 132.78, 127.56, 126.69, 116.78, 116.28, 107.33, 106.29, 102.30, 101.05, 95.93, 24.60; HRMS (ESI): *m/z*, Calcd. for $C_{18}H_{16}O_3N_5$ $[M+H]^+$: 350.1248, Found 350.1241.

4.3. Synthesis of compound 14

4.3.1. Preparation of 4-bromo-7-fluoro-2-methyl-1*H*-indole (13)

To a solution of 2-fluoro-5-bromonitrobenzene (1.0 g, 4.55 mmol) in anhydrous THF (10 mL) was added isopropenyl magnesium bromide in THF (0.5 M, 36.4 mL, 18.2 mmol) at -40 ° C under argon atmosphere. The mixture was stirred at -40 °C for 1 h, and then quenched with saturated ammonium chloride, and extracted with ethyl acetate (40 mL). Then the organic layer was washed with saturated ammonium chloride (40 mL × 2), water (20 mL × 2), dried over anhydrous magnesium sulfate, and purified by column chromatography (P/E = 50:1) to give the title compound (319 mg, 20.6%) as brown oil. ^{1}H-NMR (400 MHz, $CDCl_3$) δ (ppm): 8.16 (s, 1H), 7.11 (dd, J_1 = 8.0 Hz, J_2 = 4.0 Hz, 1H), 6.71 (dd, J_1 = 10.8 Hz, J_2 = 8.4 Hz, 1H), 6.30-6.29 (m, 1H), 2.47 (s, 3H).

4.3.2. Preparation of *N*-(3-chloro-4-fluorophenyl)-7-fluoro-2-methyl-1*H*-indol-4-amine (14a)

To a solution of compound **13** (100 mg, 0.44 mmol) in toluene (5 mL) under argon atmosphere was added $Pd_2(dba)_3$ (40 mg, 0.044 mmol), Davephos (42 mg, 0.09 mmol), K_3PO_4 (280 mg, 1.32 mmol, 1.3 mL H_2O) and 3-chloro-4-fluoroaniline (191 mg, 1.32 mmol), and then the mixture was stirred at refluxing temperature for 12 h. The mixture was cooled to room temperature, concentrated, and the residue was dissolved in ethyl acetate (10 mL). The organic layer was washed with saturated brine (10 mL × 3) and water (10 mL × 2), concentrated and purified by column chromatography (P/E = 20:1) to give the title compound (36 mg, 28.1%) as a light brown solid, mp: 103-105 □. ^{1}H-NMR (400 MHz, $CDCl_3$) δ (ppm): 8.11 (s, 1H), 6.97 (t, J = 8.8 Hz, 1H), 6.91 (dd, J_1 = 6.4 Hz, J_2 = 2.8 Hz, 1H), 6.78-6.70 (m, 3H), 6.07 (s, 1H), 2.44 (s, 3H); HRMS (ESI): *m/z*, Calcd. for $C_{15}H_{12}N_2ClF_2$ $[M+H]^+$: 293.0652, Found 293.0653.

4.3.3. Preparation of *N*-(3-chloro-4-fluorophenyl)-7-fluoro-1*H*-indol-4-amine (14b)

Compound **9a** (100 mg, 0.31 mmol), Cu (2 mg, 0.02 mmol) was added to a microwave tube, dissolved in quinoline (0.5 mL), and filled with argon gas. The microwave reaction was carried out at 240 °C for 12 min. The mixture was cooled to room temperature, concentrated, and the residue was dissolved in ethyl acetate (20 mL), washed with water (20 mL × 2), dried over anhydrous magnesium sulfate, and concentrated in vacuo and purified by column chromatography (P/E = 5:1) to give the title compound (40 mg, 46.5%) as a brown solid, mp: 73-75 □.^{1}H-NMR (400 MHz, $CDCl_3$) δ (ppm): 8.37 (brs, 1H), 7.20 (td, J_1 = 2.8 Hz, J_2 = 0.4 Hz, 1H), 6.99 (t, J = 8.8 Hz, 1H), 6.96 (dd, J_1 = 6.4 Hz, J_2 = 1.2 Hz, 1H), 6.86-6.74 (m, 3H), 6.42 (td, J_1 = 3.2 Hz, J_2 = 2.0 Hz, 1H), 5.65 (brs, 1H); HRMS (ESI): *m/z*, Calcd. for $C_{14}H_{10}N_2ClF_2$ $[M+H]^+$: 279.0495, Found 279.0497.

4.3.4. Preparation of (4-((3-chloro-4-fluorophenyl)amino)-7-fluoro-1*H*-indol-2-yl)methanol (14c)

To a solution of compound **9a** (200 mg, 0.62 mmol) in THF (5 mL) was added

borane (1M in THF, 6.2 mL, 6.2 mmol) at 0 □, and stirred for 5 h. A small amount of materials remained, and the temperature was raised to room temperature for another 3 h. The reaction was quenched by dilute hydrochloric acid, and diluted with ethyl acetate (20 mL). The mixture was washed with water (20 mL × 2), dried over anhydrous magnesium sulfate, concentrated in vacuo and purified by column chromatography (D/M = 50:1) to give the title compound (98 mg, 55.7%) as a khaki solid, mp: 101-103 □. ^{1}H-NMR (400 MHz, $CDCl_3$) δ (ppm): 8.68 (s, 1H), 6.98 (t, J = 8.8 Hz, 1H), 6.91 (dd, J_1 = 6.0 Hz, J_2 = 2.8 Hz, 1H), 6.82 (t, J = 9.6 Hz, 1H), 6.76-6.72 (m, 2H), 6.24 (s, 1H), 4.82 (s, 2H); ^{13}C-NMR (100 MHz, DMSO-d_6) δ (ppm): 150.72 (d, J = 235.1 Hz), 145.74 (d, J = 236.3 Hz), 143.54 (d, J = 1.7 Hz), 141.10, 130.58 (d, J = 2.2 Hz), 125.49 (d, J = 5.7 Hz), 125.15 (d, J = 14.5 Hz), 119.77 (d, J = 18.3 Hz), 117.44 (d, J = 21.4 Hz), 116.29, 115.49 (d, J = 6.3 Hz), 109.00 (d, J = 6.2 Hz), 106.17 (d, J = 17.4 Hz), 98.85, 57.11; HRMS (ESI): *m/z*, Calcd. for $C_{15}H_{12}ON_2ClF_2$ $[M+H]^+$: 309.0601, Found 309.0594.

4.3.5. Preparation of 4-((3-chloro-4-fluorophenyl)amino)-7-fluoro-1*H*-indole-2-carboxamide (14d)

To a solution of compound **9a** (90 mg, 0.28 mmol) in anhydrous DMF (10 mL) was added EDCI (118 mg, 0.61 mmol), HOBt (83 mg, 0.61 mmol) at room temperature, and stirred at 40 □ for 0.5 h. Then ammonium hydroxide (0.13 mL, 0.84 mmol) was added to the reaction solution, and the reaction was carried out overnight at room temperature. The reaction solution was concentrated, and the residue was dissolved in ethyl acetate (10 mL), washed with saturated sodium bicarbonate (10 mL × 3), brine (10 mL × 2), dried over anhydrous magnesium sulfate, concentrated in vacuo and purified by column chromatography (P/E = 1:1) to give the title compound (33 mg, 36.8%) as a brown solid, mp: 101-103 □. ^{1}H-NMR (500 MHz, DMSO-d_6) δ (ppm): 11.94 (s, 1H), 8.22 (s, 1H), 7.89 (brs, 1H), 7.40 (brs, 1H), 7.22 (t, J = 9.0 Hz, 1H), 7.13 (s, 1H), 7.00 (dd, J_1 = 6.0 Hz, J_2 = 2.5 Hz, 1H), 6.94 (dd, J_1 = 10.5 Hz, J_2 = 8.5 Hz, 1H), 6.89-6.87 (m, 1H), 6.73 (dd, J_1 = 8.5 Hz, J_2 = 3.5 Hz, 1H); HRMS (ESI): *m/z*, Calcd. for $C_{15}H_{11}ON_3ClF_2$ $[M+H]^+$: 322.0553, Found 322.0549.

4.3.6. Preparation of (4-((3-chloro-4-fluorophenyl)amino)-7-fluoro-1*H*-indol-2-yl)methanol (14e)

To a solution of compound **9a** (100 mg, 0.31 mmol) in anhydrous DMF (4 mL) was added EDCI (131 mg, 0.68 mmol), HOBt (92 mg, 0.68 mmol), trimethylamine (0.13 mL, 0.93 mmol) at room temperature, and stirred at 40 □ for 0.5 h. Then 50% hydroxylamine aqueous solution (62 mg, 0.93 mmol) was added to the reaction solution, and the reaction was carried out overnight at 40 □. The reaction mixture was cooled to room temperature and poured into ice water. The produced precipitate was filtered and the filter cake was purified by column chromatography (D/M = 20:1) to give the title compound (51 mg, 48.7%) as a light brown solid, mp: 151-153 □. ^{1}H-NMR (400 MHz, DMSO-d_6) δ (ppm): 12.05 (s, 1H), 11.18 (brs, 1H), 9.13 (s, 1H), 8.23 (s, 1H), 7.22 (t, J = 9.2 Hz, 1H), 7.01-6.99 (m, 2H), 6.96-6.88 (m, 2H), 6.72 (dd, J_1 = 8.0 Hz, J_2 = 3.2 Hz, 1H); HRMS (ESI): *m/z*, Calcd. for $C_{15}H_{11}O_2N_3ClF_2$ $[M+H]^+$: 338.0502, Found 338.0500.

4.3.7. Preparation of 4-bromo-7-fluoro-1*H*-indole-2-carbonitrile (15)

To a solution of compound **3a** (1.0 g, 3.5 mmol) in THF/EtOH (1:1, 20 mL) was added 1.0 M NaOH solution (17.5 mL, 17.5 mmol) dropwise and stirred at 40 □ for 5 h. The solvent was evaporated in vacuo and the residue was acidified with 1N HCl. The produced precipitate was filtered and dried to give 4-bromo-7-fluoro-1*H*-indole-2-carboxylic acid (600 mg, 99.0%) as a white solid, mp: >250 □. ^{1}H-NMR (400 MHz, DMSO-d_6) δ (ppm): 12.15 (s, 1H), 7.17 (dd, J_1 = 8.4 Hz, J_2 = 4.0 Hz, 1H), 6.93 (dd, J_1 = 10.8 Hz, J_2 = 8.4 Hz, 1H), 6.78 (t, J = 2.4 Hz, 1H).

To a solution of 4-bromo-7-fluoro-1*H*-indole-2-carboxylic acid (680 mg, 2.64 mmol) in DCM (20 mL) was added oxalyl chloride (669 mg, 5.27 mmol), DMF (1 drop) and stirred at room temperature for 2 h. Then ammonium hydroxide (2.03 mL, 13.2 mmol) was added, and the reaction mixture was stirred at room temperature overnight. The produced precipitate was filtered and dried to give

4-bromo-7-fluoro-1*H*-indole-2-carboxamide (616 mg, 90.9%) as a white solid, mp: >250 □. ^{1}H-NMR (400 MHz, DMSO-d_6) δ (ppm): 8.14 (s, 1H), 7.55 (s, 1H), 7.23 (dd, J_1 = 8.4 Hz, J_2 = 4.0 Hz, 1H), 7.22 (d, J = 3.2 Hz, 1H), 7.00 (dd, J_1 = 10.8 Hz, J_2 = 8.4 Hz, 1H).

To a solution of 4-bromo-7-fluoro-1*H*-indole-2-carboxamide (570 mg, 2.22 mmol) in toluene (10 mL) was added phosphorus oxychloride (0.83 mL, 8.87 mmol) under argon atmosphere, and stirred at refluxing temperature for 3 h. The reaction solution was cooled to room temperature and poured into a saturated aqueous solution of sodium carbonate (30 mL), and extracted with ethyl acetate (20 mL × 3). The organic layer was concentrated to give compound **15** (469 mg, 88.5%) as an off-white solid, mp: 218-220 □. ^{1}H-NMR (400 MHz, $CDCl_3$) δ (ppm): 8.88 (brs, 1H), 7.30 (dd, J_1 = 8.4 Hz, J_2 = 4.0 Hz, 1H), 7.27-7.26 (m, 1H), 7.00 (dd, J_1 = 10.4 Hz, J_2 = 8.4 Hz, 1H).

4.3.8. Preparation of 4-((3-chloro-4-fluorophenyl)amino)-7-fluoro-1*H*-indole-2-carbonitrile (14f)

Compound **15** (250 mg, 1.05 mmol), $Pd_2(dba)_3$ (96 mg, 0.105 mmol), X-phos (100 mg, 0.21 mmol), Cs_2CO_3 (1.02 g, 3.14 mmol) and 3-chloro-4-fluoroaniline (457 mg, 3.14 mmol) was added to a microwave tube, dissolved in 1,4-dioxane, and filled with argon gas. The microwave reaction was carried out at 100 °C for 0.5 h, and the starting material disappeared. The mixture was cooled to room temperature, concentrated, and the residue was dissolved in ethyl acetate (20 mL), washed with saturated brine (20 mL × 3) and water (20 mL × 2), dried over anhydrous magnesium sulfate, concentrated in vacuo and purified by column chromatography (P/E = 20:1) to give the title compound (130 mg, 40.9%) as a light yellow solid, mp: 195-197 □. ^{1}H-NMR (400 MHz, $CDCl_3$) δ (ppm): 8.72 (s, 1H), 7.09-6.99 (m, 4H), 6.85-6.82 (m, 1H), 6.78 (dd, J_1 = 8.0 Hz, J_2 = 4.0 Hz, 1H); ^{13}C-NMR (100 MHz, DMSO-d_6) δ (ppm): 151.74 (d, J = 237.1 Hz), 144.57 (d, J = 237.1 Hz), 141.66 (d, J = 2.3 Hz), 133.13 (d, J = 2.7 Hz), 126.99 (d, J = 15.8 Hz), 122.24 (d, J = 4.7 Hz), 120.04 (d, J = 18.4 Hz), 118.57, 117.74 (d, J = 19.6 Hz), 117.60 (d, J = 4.5 Hz), 114.58, 112.70 (d, J

= 1.3 Hz), 110.98 (d, *J* = 16.8 Hz), 106.53 (d, *J* = 5.7 Hz), 106.20; HRMS (ESI): m/z, Calcd for $C_{15}H_9N_3ClF_2$ $[M+H]^+$: 304.0448, Found 304.0443.

4.3.9. Preparation of 4-((3-chloro-4-fluorophenyl)amino)-7-fluoro-*N*'-hydroxy-1*H*-indole-2-carboximidamide (14g)

To a solution of compound **14f** (75 mg, 0.25 mmol) in EtOH (5 mL) was added hydroxylamine hydrochloride (86 mg, 1.23 mmol), triethylamine (0.17 mL, 1.23 mmol), and the mixture was stirred at room temperature overnight. The reaction solution was concentrated, and the residue was dissolved in ethyl acetate (10 mL), washed with water (10 mL × 2), dried over anhydrous magnesium sulfate, concentrated in vacuo and purified by column chromatography (P/E = 2:1) to give the title compound (49 mg, 59%) as a light brown solid, mp: 200-202 □. ^{1}H-NMR (400 MHz, DMSO-d_6) δ (ppm): 11.54 (s, 1H), 9.65 (s, 1H), 8.14 (s, 1H), 7.20 (t, *J* = 8.8 Hz, 1H), 6.97 (dd, J_1 = 6.4 Hz, J_2 = 2.4 Hz, 1H), 6.89-6.84 (m, 2H), 6.81 (dd, J_1 = 2.8 Hz, J_2 = 2.4 Hz, 1H), 6.70 (dd, J_1 = 8.4 Hz, J_2 = 3.6 Hz, 1H), 5.82 (s, 2H); ^{13}C-NMR (100 MHz, DMSO-d_6) δ (ppm): 150.82 (d, *J* = 235.1 Hz), 146.27, 145.68 (d, *J* = 237.8 Hz), 143.39 (d, *J* = 1.6 Hz), 132.17, 131.10 (d, *J* = 2.5 Hz), 125.53 (d, *J* = 14.6 Hz), 125.25 (d, *J* = 5.4 Hz), 119.83 (d, *J* = 18.2 Hz), 117.51 (d, *J* = 21.5 Hz), 116.37, 115.57 (d, *J* = 6.3 Hz), 109.44 (d, *J* = 6.1 Hz), 107.60 (d, *J* = 17.5 Hz), 100.20; HRMS (ESI): m/z, Calcd for $C_{15}H_{12}ON_4ClF_2$ $[M+H]^+$: 337.0662, Found 337.0666.

4.4. General procedure for preparation of 1*H*-indole-2-carboxylic acids (17a-17f)

To a solution of compound **16** in THF/EtOH (1:1) was added 1.0 M LiOH solution (5 eq) dropwise and stirred at 40 □ until the ester group was completely hydrolyzed. The solvent was evaporated in vacuo and the residue was acidified with 1N HCl. After filtration, the title compound was obtained.

4.4.1. 4-((3-Chloro-4-fluorophenyl)thio)-7-fluoro-1*H*-indole-2-carboxylic acid (17a): white solid, yield: 43.4%, mp: 171-173 □, ^{1}H-NMR (400 MHz, DMSO-d_6) δ (ppm): 13.29 (brs, 1H), 12.69 (s, 1H), 7.40-7.28 (m, 3H), 7.20-7.15 (m, 2H), 6.97 (s, 1H).

4.4.2. 4-((3-Chloro-4-fluorobenzyl)amino)-7-fluoro-1*H*-indole-2-carboxylic acid (17b): brown solid, yield: 87.0%, mp: 113-115 □, ^{1}H-NMR (400 MHz, DMSO-d_6) δ (ppm): 11.71 (s, 1H), 7.56 (dd, J_1 = 7.6 Hz, J_2 = 2.0 Hz, 1H), 7.40-7.32 (m, 3H), 6.70 (dd, J_1 = 11.2 Hz, J_2 = 8.4 Hz, 1H), 6.55 (t, J = 6.0 Hz, 1H), 5.75 (dd, J_1 = 8.4 Hz, J_2 = 2.8 Hz, 1H), 4.37 (d, J = 5.6 Hz, 2H); ^{13}C-NMR (100 MHz, DMSO-d_6) δ (ppm): 163.37, 156.46 (d, J = 243.3 Hz), 142.59 (d, J = 232.1 Hz), 138.98 (d, J = 3.4 Hz), 138.83 (d, J = 1.0 Hz), 129.76, 129.33, 128.05 (d, J = 7.2 Hz), 126.34 (d, J = 15.5 Hz), 119.99 (d, J = 4.4 Hz), 119.63 (d, J = 17.5 Hz), 117.12 (d, J = 20.6 Hz), 109.48 (d, J = 16.6 Hz), 106.58, 96.76 (d, J = 5.1 Hz), 45.85; HRMS (ESI): m/z, Calcd for $C_{16}H_{12}O_2N_2ClF_2$ $[M+H]^+$: 337.0550, Found 337.0551.

4.4.3. 4-(3-Chloro-4-fluorobenzamido)-7-fluoro-1*H*-indole-2-carboxylic acid (17c): off-white solid, yield: 76%, mp: 207-209 □, ^{1}H-NMR (400 MHz, DMSO-d_6) δ (ppm): 11.90 (brs, 1H), 10.29 (s, 1H), 8.26 (dd, J_1 = 7.2 Hz, J_2 = 2.4 Hz, 1H), 8.04 (ddd, J_1 = 8.4 Hz, J_2 = 4.8 Hz, J_3 = 2.0 Hz, 1H), 7.59 (t, J = 8.8 Hz, 1H), 7.33 (dd, J_1 = 8.4 Hz, J_2 = 4.0 Hz, 1H), 7.18 (d, J = 2.4 Hz, 1H), 6.99 (dd, J_1 = 10.8 Hz, J_2 = 8.4 Hz, 1H); HRMS (ESI): m/z, Calcd for $C_{16}H_{10}O_3N_2ClF_2$ $[M+H]^+$: 351.0343, Found 351.0339.

4.4.4. 4-((3-Chloro-4-fluorophenyl)carbamoyl)-7-fluoro-1*H*-indole-2-carboxylic acid (17d): white solid, yield: 97.1%, mp: >250 □, ^{1}H-NMR (400 MHz, DMSO-d_6) δ (ppm): 13.29 (s, 1H), 12.61 (s, 1H), 10.48 (s, 1H), 8.11 (dd, J_1 = 6.8 Hz, J_2 = 2.8 Hz, 1H), 7.74 (ddd, J_1 = 9.2 Hz, J_2 = 4.4 Hz, J_3 = 2.8 Hz, 1H), 7.68 (dd, J_1 = 8.4 Hz, J_2 = 4.4 Hz, 1H), 7.54 (dd, J_1 = 2.8 Hz, J_2 = 2.0 Hz, 1H), 7.43 (t, J = 9.2 Hz, 1H), 7.24 (dd, J_1 = 10.8 Hz, J_2 = 8.0 Hz, 1H); ^{13}C-NMR (100 MHz, DMSO-d_6) δ (ppm): 165.92, 162.74, 153.74 (d, J = 241.4 Hz), 151.66 (d, J = 251.0 Hz), 137.07 (d, J = 3.0 Hz), 131.80 (s, 1H), 129.70 (d, J = 6.5 Hz), 126.34 (d, J = 13.8 Hz), 124.66 (d, J = 3.7 Hz), 122.03, 121.94, 120.95 (d, J = 6.8 Hz), 119.48 (d, J = 18.2 Hz), 117.31 (d, J = 21.5 Hz), 109.17, 108.78 (d, J = 17.0 Hz); HRMS (ESI): m/z, Calcd for $C_{16}H_{10}O_3N_2ClF_2$ $[M+H]^+$: 351.0343, Found 351.0344.

4.4.5. 4-(2-(3-Chloro-4-fluorophenyl)acetamido)-7-fluoro-1*H*-indole-2-carboxylic acid (17e): light yellow solid, yield: 92.9%, mp: 230-232 □, ^{1}H-NMR (400 MHz,

DMSO-d_6) δ (ppm): 12.22 (s, 1H), 9.99 (s, 1H), 7.60-7.57 (m, 2H), 7.52 (s, 1H), 7.38 (d, J = 7.2 Hz, 2H), 6.97 (dd, J_1 = 11.2 Hz, J_2 = 8.4 Hz, 1H), 3.81 (s, 2H); ^{13}C-NMR (100 MHz, DMSO-d_6) δ (ppm): 169.23, 163.03, 156.63 (d, J = 243.6 Hz), 146.28 (d, J = 241.3 Hz), 134.56 (d, J = 3.7 Hz), 131.68, 130.58, 130.36 (d, J = 7.2 Hz), 128.50 (d, J = 3.0 Hz), 126.21 (d, J = 15.0 Hz), 123.63 (d, J = 5.2 Hz), 119.47 (d, J = 17.5 Hz), 117.13 (d, J = 20.6 Hz), 110.94 (d, J = 5.7 Hz), 108.94 (d, J = 16.9 Hz), 106.81, 41.92; HRMS (ESI): m/z, Calcd for $C_{17}H_{12}O_3N_2ClF_2$ $[M+H]^+$: 365.0499, Found 365.0494.

4.4.6. 4-(3-(3-Chloro-4-fluorophenyl)ureido)-7-fluoro-1*H*-indole-2-carboxylic acid (17f): white solid, yield: 95.2%, mp: >250 □, ^{1}H-NMR (400 MHz, CD_3OD) δ 7.75 (dd, J_1 = 6.4 Hz, J_2 = 2.4 Hz, 1H), 7.46 (dd, J_1 = 8.4 Hz, J_2 = 3.6 Hz, 1H), 7.30 (ddd, J_1 = 8.8 Hz, J_2 = 4.0 Hz, J_3 = 2.8 Hz, 1H), 7.26 (d, J = 2.4 Hz, 1H), 7.17 (t, J = 8.8 Hz, 1H), 6.93 (dd, J_1 = 10.8 Hz, J_2 = 8.4 Hz, 1H); HRMS (ESI): m/z, Calcd for $C_{16}H_{11}O_3N_3ClF_2$ $[M+H]^+$: 366.0452, Found 366.0448.

4.5. Synthesis of compound 9p-O

4.5.1. Preparation of ethyl 4-((3-chloro-4-fluorophenyl)imino)-6-(ethylamino)-7-oxo-4,7-dihydro-1*H*-indole-2-carboxylate (8p-O)

To a solution of compound **8p** (100 mg, 0.27 mmol) in DCM（5 mL）was added *m*-chloroperoxybenzoic acid (70 mg, 0.41 mmol) dropwise at 0 ℃. The reaction mixture was stirred for 1 h. The reaction solution was dilute with DCM (30 mL), washed with saturated sodium carbonate solution (30 mL × 2), water (30 mL × 2), dried over anhydrous magnesium sulfate, concentrated in vacuo and purified by column chromatography (P/E = 10:1) to give the title compound (84 mg, 81%) as a brown solid, mp: >250 ℃. ^{1}H-NMR (400 MHz, $CDCl_3$) δ (ppm): 9.99 (s, 1H), 7.40 (s, 1H), 7.14 (t, J = 8.8 Hz, 1H), 7.02 (s, 1H), 6.82 (s, 1H), 5.48 (s, 1H), 5.41 (s, 1H), 4.40 (q, J = 7.2 Hz, 2H), 3.05-2.99 (m, 2H), 1.39 (t, J = 7.2 Hz, 3H), 1.26 (t, J = 7.2 Hz, 3H).

4.5.2. Preparation of 4-((3-chloro-4-fluorophenyl)imino)-6-(ethylamino)-7-oxo-4,7-dihydro-1*H*-indole-2-carboxylate (9p-O)

To a solution of compound **8p-O** (80 mg, 0.21 mmol) in THF (1 mL) was added 1.0 M LiOH solution (1.03 mL, 1.05 mmol) dropwise and stirred at refluxing temperature for 8 h. A small amount of the starting material remained, and the remaining material was washed away by diethyl ether (5 mL). The water phase was acidified with 1N HCl. After filtration and dried, the filter cake was purified by column chromatography (D/M = 20:1) to give the title compound (44 mg, 59.5%) as a black solid, mp: >250 □. ^{1}H-NMR (400 MHz, DMSO-d_6) δ (ppm): 13.59 (brs, 2H), 7.54-7.49 (m, 3H), 7.22 (s, 1H), 5.39 (s, 1H), 3.14 (s, 2H), 1.10 (t, J = 7.2 Hz, 3H); HRMS (ESI): m/z, Calcd for $C_{17}H_{14}O_3N_3ClF$ $[M+H]^+$: 362.0702, Found 362.0702.

Note: The following information and data were listed in the supplementary information, including the synthesis and characterization of all intermediates (except for the target compounds shown in **Tables 1-4**) in the **Schemes 1-4**, the ^{1}H-NMR spectra of all target compounds and ^{13}C-NMR spectra of some target compounds, and the X-ray diffraction data of compound **8p-O**.

4.6 Biological evaluation

4.6.1. The enzymatic assay for IDO1 and TDO inhibition

Recombinant human IDO1 and TDO were expressed and purified according to the reported protocol [49]. The assay for IDO1 and TDO inhibition was performed according to the literature [50]: A standard reaction mixture (100 μL) containing 100 mM potassium phosphate buffer (pH 6.5), 40 mM ascorbic acid (neutralized with NaOH), 200 μg/mL catalase, 20 μM methylene blue and 0.05 μM rhIDO1 or rhTDO was added to the solution containing the substrate L-tryptophan and the test sample at a determined concentration. The reaction was carried out at 37 ºC for 45 min and stopped by adding 20 μL of 30% (w/v) trichloroacetic acid. After heating at 65 ºC for 15 min, 100 μL of 2% (w/v) *p*-dimethylaminobenzaldehyde in acetic acid was added to each well. The yellow pigment derived from kynurenine was measured at 490 nm using a SYNERGY-H1 microplate reader (Biotek Instruments, Inc., Winooski, VT, USA). IC_{50} was analyzed using the GraphPad Prism 8.0 software (GraphPad Software,

San Diego, CA, USA).

4.6.2. Cellular IDO1/TDO inhibition assay

Cellular IDO1/TDO inhibition assay was performed as previously described [49]. First, 4×10^4 A172 cells were inoculated in a 96-well plate with a volume of 100 μL. The next day, a solution containing the test compound in a medium of 10% serum was perpared, the final concentration of IFNγ was 100 ng/mL, and the final concentration of substrate Trp was 1 mmol/L. The prepared solution was added to A172 cells, and incubated for 48 hours followed by taking the supernatant for detection. 100 μL of supernatant was added to a new 96-well plate, and the protein reaction was stopped by adding 20 μL of 30% (w/v) trichloroacetic acid. After heating at 65 ºC for 15 min, 100 μL of 2% (w/v) *p*-dimethylaminobenzaldehyde in acetic acid was added to each well. The yellow pigment derived from kynurenine was measured at 490 nm using a SYNERGY-H1 microplate reader (Biotek Instruments, Inc., Winooski, VT, USA). The IC_{50} value was calculated using the GraphPad Prism 8.0 software (GraphPad Software, San Diego, CA, USA).

4.6.3. T Cell Proliferation Assay

T cell proliferation assay was performed as previously described [17] with some modifications. T lymphocytes prepared from splenocytes of BALB/c mice were resuspended in RPMI 1640 containing 10% FBS, L-glutamate, penicillin, and streptomycin. The LLC cells were treated with mitomycin C at a final concentration of 25 μg/mL and then incubated at 37 °C for 1 h. After being washed three times, the LLC cells were resuspended in RPMI 1640. 1×10^5 T lymphocytes (responder cells), 1×10^4 mitomycin C treated LLC cells (stimulator cells) and test compounds were added to each well of a 96-well plate. The plates were incubated at 37 °C and 5% CO_2 for 3 days. Then the cell proliferation was quantified by CellTiter-Glo® Luminescent Cell Viability Assay (Promega, USA) according to the protocol.

4.6.4. The in vivo antitumor activity assay

C57BL/6 mice were obtained from Beijing Vital River Laboratory Animal

Technology Co., Ltd. (Beijing Vital River Laboratory Animal Technology Co., Ltd, Beijing, China). Studies involving mice were approved by the Experimental Animal Management and Welfare Committee at the Institute of Materia Medica, Peking Union Medical College.

The mouse melanoma cells B16F10 were cultured and harvested in saline. At day 0 of the experiment, 1×10^6 cells were injected subcutaneously into mice, and treatment was initiated at day 1 following the mice enrolled randomly in control and experimental groups. For control group, 0.5% CMC-Na was orally administered every day. Compound **9o-23** was dissolved in 0.5% CMC-Na for oral treatment. When the mice were sacrificed, the tumors were stripped and weighted. The tumor growth inhibition (TGI) was calculated as TGI = (1 - tumor $\text{weight}_{\text{treatment}}$/tumor $\text{weight}_{\text{vehicle}}$) × 100%. The statistical analysis was performed with GraphPad Prism 8.0 software and the significance level was evaluated with a one-way ANOVA model. [47]

4.7. Computational studies

All molecular computation studies were performed using CDOCKER protocol integrated in Accelrys Discovery Studio Client 2018 (Accelrys Software Inc., San Diego, CA). The co-crystal structures of Trp-IDO1 complex (PDB ID: 5WMU, chain A) and Trp-TDO complex (PDB ID: 5TIA, chain A and B) were chosen for molecular modeling. The docking protocol of compound **9o** with IDO1 and TDO were chosen as representatives. Using Prepare Protein tool of DS, the water molecules in protein were removed and the protein were added hydrogens, corrected the incomplete residues and refined with CHARMm force field. Trp was chosen as the center to construct the binding site within 9 Å. Compound **9o** was minimized using Prepare Ligands tool of DS and refined with CHARMm forcefield. Then it was docked into the prepared IDO1 and TDO protein with CDOCKER using the default parameters, respectively. The 20 final docked conformations were ranked according to their binding free energy. The docking mode was chosen on the basis of binding rationality, and then molecular dynamics simulation was performed to further optimize the binding pose of compond **9o** within the binding pocket of each enzyme.

Small molecules were assigned with AM1BCC partial charges and extracted into frcmod files using the AmberTools16 program Antechamber and Parmchk2. The heme parameter (all-atom) was downloaded from Bryce Group AMBER parameter database (http://research.bmh.manchester.ac.uk/bryce/amber). Then, protein-ligand complex PDB files were solvated in a water (TIP3P) octahedron. The minimum distance between any atom of protein complex and the edge of the periodic box was set to 1.2 nm with a 1.0 nm cutoff. Amber 16 package was used to carry out MD simulation at a temperature of 310 K for a 30 ns process with force fields ff14SB and gaff. RMSD (Root Mean Square Deviation) was caculated with cpptraj, and the first MD frame was used as the reference [51].

Acknowledgements

This work is supported by CAMS Initiative for Innovative Medicine (CAMS-I2M-2-004) and National Science & Technology Major Project Key New Drug Creation and Manufacturing Program, China (2018ZX09711001-003).

References

[1] N. van Baren, B.J. Van den Eynde, Tryptophan-degrading enzymes in tumoral immune resistance, Front. Immunol. 6 (2015). https://doi.org/10.3389/fimmu.2015.00034.

[2] Z. Ye, L. Yue, J. Shi, M. Shao, T. Wu, Role of IDO and TDO in Cancers and Related Diseases and the Therapeutic Implications, J. Cancer. 10 (2019) 2771–2782. doi:10.7150/jca.31727.

[3] A.F. Abdel-Magid, Targeting the Inhibition of Tryptophan 2,3-Dioxygenase (TDO-2) for Cancer Treatment, ACS Med. Chem. Lett. 8 (2017) 11–13. https://doi.org/10.1021/acsmedchemlett.6b00458

[4] F. Fallarino, U. Grohmann, K.W. Hwang, C. Orabona, C. Vacca, R. Bianchi, M.L. Belladonna, M.C. Fioretti, M.L. Alegre, P. Puccetti, Modulation of tryptophan catabolism by regulatory T cells, Nat. Immunol. 4 (2003) 1206–1212. http://dx.doi.org/10.1038/ni1003-1037.

[5] D. Wang, Y. Saga, H. Mizukami, N. Sato, H. Nonaka, H. Fujiwara, Y. Takei, S. Machida, O. Takikawa, K. Ozawa, M. Suzuki, Indoleamine-2,3-dioxygenase, an immunosuppressive enzyme that inhibits natural killer cell function, as a useful target for ovarian cancer

therapy, Int. J. Oncol. 40 (2012) 929–934. doi:10.3892/ijo.2011.1295.

[6] G.C. Prendergast, W.J. Malachowski, A. Mondal, P. Scherle, A.J. Muller, Indoleamine 2,3-Dioxygenase and Its Therapeutic Inhibition in Cancer, 1st ed., Elsevier Inc., 2018. https://doi.org/10.1016/bs.ircmb.2017.07.004

[7] N.J.C. King, S.R. Thomas, Molecules in focus: Indoleamine 2,3-dioxygenase, Int. J. Biochem. Cell Biol. 39 (2007) 2167–2172. https://doi.org/10.1016/j.biocel.2007.01.004.

[8] A. Lewis-Ballester, F. Forouhar, S.M. Kim, S. Lew, Y. Wang, S. Karkashon, J. Seetharaman, D. Batabyal, B.Y. Chiang, M. Hussain, M.A. Correia, S.R. Yeh, L. Tong, Molecular basis for catalysis and substrate-mediated cellular stabilization of human tryptophan 2,3-dioxygenase, Sci. Rep. 6 (2016) 1–13. doi:10.1038/srep35169.

[9] N. Chauhan, J. Basran, S.A. Rafice, I. Efimov, E.S. Millett, C.G. Mowat, P.C.E. Moody, S. Handa, E.L. Raven, How is the distal pocket of a heme protein optimized for binding of tryptophan?, FEBS J. 279 (2012) 4501–4509. https://doi.org/10.1111/febs.12036.

[10] H. Sugimoto, S.I. Oda, T. Otsuki, T. Hino, T. Yoshida, Y. Shiro, Crystal structure of human indoleamine 2,3-dioxygenase: Catalytic mechanism of O2 incorporation by a heme-containing dioxygenase, Proc. Natl. Acad. Sci. U. S. A. 103 (2006) 2611–2616. https://doi. 10.1073/pnas.0508996103.

[11] T. Weng, X. Qiu, J. Wang, Z. Li, J. Bian, Recent discovery of indoleamine-2,3-dioxygenase 1 inhibitors targeting cancer immunotherapy, Eur. J. Med. Chem. 143 (2018) 656–669. https://doi.org/10.1016/j.ejmech.2017.11.088.

[12] J.E. Cheong, L. Sun, Targeting the IDO1/TDO2–KYN–AhR Pathway for Cancer Immunotherapy – Challenges and Opportunities, Trends Pharmacol. Sci. 39 (2018) 307–325. https://doi.org/10.1016/j.tips.2017.11.007.

[13] J.E. Cheong, A. Ekkati, L. Sun, A patent review of IDO1 inhibitors for cancer, Expert Opin. Ther. Pat. 28 (2018) 317–330. https://doi.org/10.1080/13543776.2018.1441290.

[14] G.C. Prendergast, W.P. Malachowski, J.B. DuHadaway, A.J. Muller, Discovery of IDO1 Inhibitors: From bench to bedside, Cancer Res. 77 (2017) 6795–6811. doi:10.1158/0008-5472.CAN-17-2285.

[15] A. Coletti, F.A. Greco, D. Dolciami, E. Camaioni, R. Sardella, M.T. Pallotta, C. Volpi, C. Orabona, U. Grohmann, A. Macchiarulo, Advances in Indolemine 2,3-Dioxygenase 1 Medicinal Chemistry: Structure-Function and Structure-Activity Relationships of the Enzyme and its Inhibitors, Medchemcomm. 8 (2017) 1378–1392. doi:10.1039/c7md00109f.

[16] U.F. Röhrig, S.R. Majjigapu, P. Vogel, V. Zoete, O. Michielin, Challenges in the Discovery of Indoleamine 2,3-Dioxygenase 1 (IDO1) Inhibitors, J. Med. Chem. 58 (2015) 9421–9437. https://doi.org/10.1021/acs.jmedchem.5b00326.

[17] S. Yang, X. Li, F. Hu, Y. Li, Y. Yang, J. Yan, C. Kuang, Q. Yang, Discovery of tryptanthrin derivatives as potent inhibitors of indoleamine 2,3-dioxygenase with therapeutic activity in lewis lung cancer (LLC) tumor-bearing mice, J. Med. Chem. 56 (2013) 8321–8331. https://doi.org/10.1021/jm401195n.

[18] R. Guda, S. Narsimha, R. Babu, S. Muthadi, H. Lingabathula, R. Palabindela, N.R. Yellu, G. Kumar, M. Kasula, Novel substituted hydrazono indolo[2,1-b]quinazoline-6,12-dione analogues as cytostatic agents: Synthesis, crystal structure, biological evaluation and molecular docking studies, Bioorganic Med. Chem. Lett. 26 (2016) 5517–5523. https://doi.org/10.1016/j.bmcl.2016.10.006.

[19] S. Paul, A. Roy, S.J. Deka, S. Panda, V. Trivedi, D. Manna, Nitrobenzofurazan derivatives of N′-hydroxyamidines as potent inhibitors of indoleamine-2,3-dioxygenase 1, Eur. J. Med. Chem. 121 (2016) 364–375. https://doi.org/10.1016/j.ejmech.2016.05.061.

[20] W.P. Malachowski, M. Winters, J.B. DuHadaway, A. Lewis-Ballester, S. Badir, J. Wai, M. Rahman, E. Sheikh, J.M. LaLonde, S.R. Yeh, G.C. Prendergast, A.J. Muller, O-alkylhydroxylamines as rationally-designed mechanism-based inhibitors of indoleamine 2,3-dioxygenase-1, Eur. J. Med. Chem. 108 (2016) 564–576. https://doi.org/10.1016/j.ejmech.2015.12.028.

[21] Z. Shiokawa, E. Kashiwabara, D. Yoshidome, K. Fukase, S. Inuki, Y. Fujimoto, Discovery of a Novel Scaffold as an Indoleamine 2,3-Dioxygenase 1 (IDO1) Inhibitor Based on the Pyrrolopiperazinone Alkaloid, Longamide B, ChemMedChem. 11 (2016) 2682–2689. https://doi.org/10.1002/cmdc.201600446.

[22] S. Panda, A. Roy, S.J. Deka, V. Trivedi, D. Manna, Fused Heterocyclic Compounds as Potent Indoleamine-2,3-dioxygenase 1 Inhibitors, ACS Med. Chem. Lett. 7 (2016) 1167–1172. https://doi.org/10.1021/acsmedchemlett.6b00359.

[23] M.G. Brant, J. Goodwin-Tindall, K.R. Stover, P.M. Stafford, F. Wu, A.R. Meek, P. Schiavini, S. Wohnig, D.F. Weaver, Identification of Potent Indoleamine 2,3-Dioxygenase 1 (IDO1) Inhibitors Based on a Phenylimidazole Scaffold, ACS Med. Chem. Lett. 9 (2018) 131–136. https://doi.org/10.1021/acsmedchemlett.7b00488.

[24] M. Serafini, E. Torre, S. Aprile, A. Massarotti, S. Fallarini, T. Pirali, Synthesis, Docking and Biological Evaluation of a Novel Class of Imidazothiazoles as IDO1 Inhibitors, (2019) 1874–1884. https://doi.org/10.3390/molecules24101874.

[25] S. Tojo, T. Kohno, T. Tanaka, S. Kamioka, Y. Ota, T. Ishii, K. Kamimoto, S. Asano, Y. Isobe, Crystal structures and structure-activity relationships of imidazothiazole derivatives as IDO1 inhibitors, ACS Med. Chem. Lett. 5 (2014) 1119–1123. https://doi.org/10.1021/ml500247w.

[26] E.W. Yue, B. Douty, B. Wayland, M. Bower, X. Liu, L. Leffet, Q. Wang, K.J. Bowman, M.J. Hansbury, C. Liu, M. Wei, Y. Li, R. Wynn, T.C. Burn, H.K. Koblish, J.S. Fridman, B. Metcalf, P.A. Scherle, A.P. Combs, Discovery of potent competitive inhibitors of indoleamine 2,3-dioxygenase with in vivo pharmacodynamic activity and efficacy in a mouse melanoma model, J. Med. Chem. 52 (2009) 7364–7367. https://doi.org/10.1021/jm900518f.

[27] E.W. Yue, R. Sparks, P. Polam, D. Modi, B. Douty, B. Wayland, B. Glass, A. Takvorian, J. Glenn, W. Zhu, M. Bower, X. Liu, L. Leffet, Q. Wang, K.J. Bowman, M.J. Hansbury, M. Wei, Y. Li, R. Wynn, T.C. Burn, H.K. Koblish, J.S. Fridman, T. Emm, P.A. Scherle, B. Metcalf, A.P. Combs, INCB24360 (Epacadostat), a Highly Potent and Selective Indoleamine-2,3-dioxygenase 1 (IDO1) Inhibitor for Immuno-oncology, ACS Med. Chem. Lett. 8 (2017) 486–491. https://doi.org/10.1021/acsmedchemlett.6b00391.

[28] M.T. Nelp, P.A. Kates, J.T. Hunt, J.A. Newitt, A. Balog, D. Maley, X. Zhu, L. Abell, A. Allentoff, R. Borzilleri, H.A. Lewis, Z. Lin, S.P. Seitz, C. Yan, J.T. Groves, Immune-modulating enzyme indoleamine 2,3-dioxygenase is effectively inhibited by targeting its apo-form, Proc. Natl. Acad. Sci. U. S. A. 115 (2018) 3249–3254. https://doi.org/10.1073/pnas.1719190115.

[29] H.H. Soliman, E. Jackson, T. Neuger, E. Claire Dees, R. Donald Harvey, H. Han, R. Ismail-Khan, S. Minton, N.N. Vahanian, C. Link, D.M. Sullivan, S. Antonia, A first in man phase I trial of the oral immunomodulator, indoximod, combined with docetaxel in patients with metastatic solid tumors, Oncotarget. 5 (2014) 8136–8146. https://doi.org/10.18632/oncotarget.2357.

[30] S. Crosignani, P. Bingham, P. Bottemanne, H. Cannelle, S. Cauwenberghs, M. Cordonnier, D. Dalvie, F. Deroose, J.L. Feng, B. Gomes, S. Greasley, S.E. Kaiser, M. Kraus, M. Négrerie, K. Maegley, N. Miller, B.W. Murray, M. Schneider, J. Soloweij, A.E. Stewart, J. Tumang, V.R. Torti, B. Van Den Eynde, M. Wythes, Discovery of a Novel and Selective Indoleamine 2,3-Dioxygenase (IDO-1) Inhibitor 3-(5-Fluoro-1H-indol-3-yl)pyrrolidine-2,5-dione (EOS200271/PF-06840003) and Its Characterization as a Potential Clinical Candidate, J. Med. Chem. 60 (2017) 9617–9629. https://doi.org/10.1021/acs.jmedchem.7b00974.

[31] A. Nayak, Z. Hao, R. Sadek, N. Vahanian, W. Ramsey, E. Kennedy, M. Mautino, C. Link,

P. Bourbo, R. Dobbins, K. Adams, A. Diamond, L. Marshall, D.H. Munn, J. Janik, S.N. Khleif, A Phase I study of NLG919 for adult patients with recurrent advanced solid tumors, J. Immunother. Cancer. 2 (2014) P250. doi:10.1186/2051-1426-2-s3-p250.

[32] E. Dolušić, P. Larrieu, L. Moineaux, V. Stroobant, L. Pilotte, D. Colau, L. Pochet, B. Van Den Eynde, B. Masereel, J. Wouters, R. Frédérick, Tryptophan 2,3-dioxygenase (TDO) inhibitors. 3-(2-(pyridyl)ethenyl)indoles as potential anticancer immunomodulators, J. Med. Chem. 54 (2011) 5320–5334. https://doi.org/10.1021/jm2006782.

[33] S. Hua, F. Chen, X. Wang, Y. Wang, S. Gou, Pt(IV) hybrids containing a TDO inhibitor serve as potential anticancer immunomodulators, J. Inorg. Biochem. 195 (2019) 130–140. https://doi.org/10.1016/j.jinorgbio.2019.02.004.

[34] C.P. Yu, Y.L. Song, Z.M. Zhu, B. Huang, Y.Q. Xiao, D.Y. Luo, Targeting TDO in cancer immunotherapy, Med. Oncol. 34 (2017) 1–9. doi:10.1007/s12032-017-0933-2.

[35] S. Zhang, F. Qi, X. Fang, D. Yang, H. Hu, Q. Huang, C. Kuang, Q. Yang, Tryptophan 2,3-dioxygenase inhibitory activities of tryptanthrin derivatives, Eur. J. Med. Chem. 160 (2018) 133–145. https://doi.org/10.1016/j.ejmech.2018.10.017.

[36] J.S. Wu, S.Y. Lin, F.Y. Liao, W.C. Hsiao, L.C. Lee, Y.H. Peng, C.L. Hsieh, M.H. Wu, J.S. Song, A. Yueh, C.H. Chen, S.H. Yeh, C.Y. Liu, S.Y. Lin, T.K. Yeh, J.T.A. Hsu, C. Shih, S.H. Ueng, M.S. Hung, S.Y. Wu, Identification of Substituted Naphthotriazolediones as Novel Tryptophan 2,3-Dioxygenase (TDO) Inhibitors through Structure-Based Virtual Screening, J. Med. Chem. 58 (2015) 7807–7819. https://doi.org/10.1021/acs.jmedchem.5b00921.

[37] Z. Pei, R. Mendonca, L. Gazzard, R. Pastor, L. Goon, A. Gustafson, E. Vanderporten, G. Hatzivassiliou, K. Dement, R. Cass, P.W. Yuen, Y. Zhang, G. Wu, X. Lin, Y. Liu, B.D. Sellers, Aminoisoxazoles as Potent Inhibitors of Tryptophan 2,3-Dioxygenase 2 (TDO2), ACS Med. Chem. Lett. 9 (2018) 417–421. https://doi.org/10.1021/acsmedchemlett.7b00427.

[38] G. V Long, R. Dummer, O. Hamid, T.F. Gajewski, C. Caglevic, S. Dalle, A. Arance, M.S. Carlino, J.-J. Grob, T.M. Kim, L. Demidov, C. Robert, J. Larkin, J.R. Anderson, J. Maleski, M. Jones, S.J. Diede, T.C. Mitchell, Epacadostat plus pembrolizumab versus placebo plus pembrolizumab in patients with unresectable or metastatic melanoma (ECHO-301/KEYNOTE-252): a phase 3, randomised, double-blind study, Lancet Oncol. 20 (2019) 1083–1097. doi:10.1016/s1470-2045(19)30274-8.

[39] M. Winters, J.B. DuHadaway, K.N. Pham, A. Lewis-Ballester, S. Badir, J. Wai, E. Sheikh, S.R. Yeh, G.C. Prendergast, A.J. Muller, W.P. Malachowski, Diaryl hydroxylamines as

pan or dual inhibitors of indoleamine 2,3-dioxygenase-1, indoleamine 2,3-dioxygenase-2 and tryptophan dioxygenase, Eur. J. Med. Chem. 162 (2019) 455–464. https://doi.org/10.1016/j.ejmech.2018.11.010.

[40] L. Yang, Y. Chen, J. He, E.M. Njoya, J. Chen, S. Liu, C. Xie, W. Huang, F. Wang, Z. Wang, Y. Li, S. Qian, 4,6-Substituted-1H-Indazoles as potent IDO1/TDO dual inhibitors, Bioorganic Med. Chem. 27 (2019) 1087–1098. https://doi.org/10.1016/j.bmc.2019.02.014.

[41] X.H. Liu, H. Park, J.H. Hu, Y. Hu, Q.L. Zhang, B.L. Wang, B. Sun, K.S. Yeung, F.L. Zhang, J.Q. Yu, Diverse ortho-C(sp^2)-H functionalization of benzaldehydes using transient directing groups, J. Am. Chem. Soc. 139 (2017) 888–896. https://doi.org/10.1021/jacs.6b11188.

[42] S.N. Gockel, K.L. Hull, Chloroform as a Carbon Monoxide Precursor: In or Ex Situ Generation of CO for Pd-Catalyzed Aminocarbonylations, Org. Lett. 17 (2015) 3236–3239. https://doi.org/10.1021/acs.orglett.5b01385.

[43] A.C. Terentis, M. Freewan, T.S. Sempértegui Plaza, M.J. Raftery, R. Stocker, S.R. Thomas, The selenazal drug ebselen potently inhibits indoleamine 2,3-dioxygenase by targeting enzyme cysteine residues, Biochemistry. 49 (2010) 591–600. https://doi.org/10.1021/bi901546e.

[44] A. Lewis-Ballester, K.N. Pham, D. Batabyal, S. Karkashon, J.B. Bonanno, T.L. Poulos, S.R. Yeh, Structural insights into substrate and inhibitor binding sites in human indoleamine 2,3-dioxygenase, Nat. Commun. 8 (2017) 1–7. doi:10.1038/s41467-017-01725-8.

[45] G. Wu, D.H. Robertson, C.L.B. Iii, M. Vieth, Detailed Analysis of Grid-Based Molecular Docking: A Case Study of CDOCKER—A CHARMm-Based MD Docking Algorithm, J. Comput. Chem. 24 (2003) 1549–1562. https://doi.org/10.1002/jcc.10306.

[46] X. Yang, F. Lyakurwa, H. Xie, J. Chen, X. Li, X. Qiao, X. Cai, Different binding mechanisms of neutral and anionic poly-/perfluorinated chemicals to human transthyretin revealed by In silico models, Chemosphere. 182 (2017) 574–583. https://doi.org/10.1016/j.chemosphere.2017.05.016.

[47] H. Sugimoto, S.I. Oda, T. Otsuki, T. Hino, T. Yoshida, Y. Shiro, Crystal structure of human indoleamine 2,3-dioxygenase: Catalytic mechanism of O2 incorporation by a heme-containing dioxygenase, Proc. Natl. Acad. Sci. U. S. A. 103 (2006) 2611–2616. https://doi.org/10.1073/pnas.0508996103.

[48] H.K. Koblish, M.J. Hansbury, K.J. Bowman, G. Yang, C.L. Neilan, P.J. Haley, T.C. Burn, P. Waeltz, R.B. Sparks, E.W. Yue, A.P. Combs, P.A. Scherle, K. Vaddi, J.S. Fridman,

Hydroxyamidine inhibitors of indoleamine-2,3-dioxygenase potently suppress systemic tryptophan catabolism and the growth of IDO-expressing tumors, Mol. Cancer Ther. 9 (2010) 489–498. doi:10.1158/1535-7163.MCT-09-0628.

[49] LAI Fang-fang, XUE Ni-na, JI Ming, DU Ting-ting, LI Ling, SHENG Li, CHEN Xiao-guang, Establishment and optimization of an enzyme-cell based high- throughput screening platform for IDO1 inhibitors, Acta Pharm. Sin. 54 (2019) 1868–1874. doi:10.16438/j.0513-4870.2019-0697.

[50] H. Wen, Y. Liu, S. Wang, T. Wang, G. Zhang, X. Chen, Y. Li, H. Cui, F. Lai, L. Sheng, Design and synthesis of indoleamine 2,3-dioxygenase 1 inhibitors and evaluation of their use as anti-tumor agents, Molecules. 24 (2019) 2124-2150. https://doi.org/10.3390/molecules24112124.

[51] D.R. Roe, T.E. Cheatham, PTRAJ and CPPTRAJ: Software for processing and analysis of molecular dynamics trajectory data, J. Chem. Theory Comput. 9 (2013) 3084–3095. https://doi.org/10.1021/ct400341p.

Highlights:

► Indole-2-carboxylic acid derivatives were synthesized as novel IDO1/TDO dual inhibitors.
► Structure-activity relationships were explored.
► Compound 9o-23 demonstrated in vivo antitumor activity.

Declaration of interests

☐ √ The authors declare that they have no known competing financial interests or personal relationships that could have appeared to influence the work reported in this paper.

☐The authors declare the following financial interests/personal relationships which may be considered as potential competing interests: